EVIR: chimeric receptors that enhance dendritic cell cross-dressing with tumor antigens

Mario Leonardo Squadrito, Chiara Cianciaruso, Sarah K Hansen & Michele De Palma

We describe a lentivirus-encoded chimeric receptor, termed extracellular vesicle (EV)-internalizing receptor (EVIR), which enables the selective uptake of cancer-cell-derived EVs by dendritic cells (DCs). The EVIR enhances DC presentation of EV-associated tumor antigens to CD8$^+$ T cells primarily through MHCI recycling and cross-dressing. EVIRs should facilitate exploring the mechanisms and implications of horizontal transfer of tumor antigens to antigen-presenting cells.

Virtually all cell types produce EVs encompassing exosomes and other microvesicles[1,2]. Tumor-derived EVs modulate cancer-associated processes, such as immunity and metastasis, by interacting with various cell types, both locally in the tumor microenvironment and via the systemic circulation in remote organs[2,3]. EVs may also deliver tumor antigens (TAs) to dendritic cells (DCs); however, the mechanistic underpinnings of this phenomenon are poorly understood[4–7].

In order to examine the process of EV-mediated TA transfer to DCs, we designed a chimeric receptor, termed EVIR, which endows DCs with the capacity to specifically recognize cancer-cell-derived EVs. The EVIR encompasses a truncated (nonsignaling) low-affinity nerve growth factor receptor (dLNGFR) and an extracellular antibody domain (**Fig. 1a**). The latter comprises an IgK signal peptide and a single-chain $F(ab)_2$ variable fragment (scFv) with specificity for the human HER2 protein, which is overexpressed in a subset of human breast cancers[8]. A hinge domain derived from dLNGFR connects the transmembrane and extracellular domains of the EVIR. We also generated a nonfunctional EVIR lacking the scFv domain, hereon referred to as control receptor (CtrlR).

We used a bidirectional lentiviral vector (LV)[9] to express the EVIR (or CtrlR) and a green fluorescent protein (GFP) transgene (**Supplementary Fig. 1a**). Anti-scFv staining of immortalized mouse bone marrow macrophages (iBMMs)[10] transduced with the EVIR-encoding LV (iBMM-EVIR) showed efficient and sustained cell-surface expression of the EVIR (**Fig. 1b** and **Supplementary Fig. 1b**,**c**).

In a cell-suspension assay, mouse P388D1 monocytes transduced with the EVIR (Mo-EVIR) readily adhered to HER2$^+$, but not HER2-negative, MC38 colorectal cancer cells fluorescently labeled with mCherry (MC38–HER2/mCh and MC38–mCh, respectively; **Fig. 1c** and **Supplementary Fig. 2a**–**c**). We also observed cell aggregation when we cultured iBMM-EVIR with HER2$^+$ MC38 cells for 24 h under adherent conditions (**Supplementary Fig. 2a**,**d**). Of note, the aggregation of MC38-HER2 (labeled with mTurquoise2, mTq) and iBMM-EVIR (labeled with GFP) did not promote the unspecific coaggregation of iBMM (labeled with mCh) in mixed cultures. Thus, an anti-HER2 EVIR specifically and efficiently binds to HER2 expressed on the surface of cancer cells.

To examine whether the EVIR enhances the uptake of HER2$^+$ EVs by BM-derived DCs (BMDCs), we exposed EVIR- and CtrlR-expressing DCs (DC-EVIR and DC-CtrlR, respectively; **Supplementary Fig. 3a**) to EVs isolated from either HER2$^+$ or HER2-negative MC38–mCh cells (EV–HER2/mCh and EV–mCh, respectively; **Supplementary Fig. 3b**,**c**). EV–HER2/mCh transferred mCh fluorescence to DC-EVIR more efficiently than EV–mCh (**Supplementary Fig. 3d**). Moreover, DC-EVIR acquired mCh fluorescence from EV–HER2/mCh more efficiently than DC-CtrlR (**Fig. 1d** and **Supplementary Fig. 3e**,**f**). Over time, the mCh fluorescence pattern transitioned from membrane associated, to largely punctate in the cytoplasm, to broadly diffuse in the cytoplasm; this kinetics appeared faster in DC-EVIR (**Supplementary Fig. 4a**). Furthermore, matched amounts of EVs isolated from MC38–mTq cells (EV–mTq) did not impair the ability of iBMM-EVIR to acquire mCh fluorescence from EV–HER2/mCh (**Supplementary Fig. 4b**), which suggested that an anti-HER2 EVIR can efficiently bind to, and internalize, EV-HER2 also in the presence of competing doses of HER2-negative EVs.

To investigate whether the anti-HER2 EVIR improves the presentation of TAs by DCs, we performed T-cell proliferation assays. We cultured CD8$^+$ OT-I T cells, which recognize the chicken ovalbumin (OVA)-derived SIINFEKL peptide loaded onto H-2Kb/B2M major histocompatibility class I (MHCI) complex[11], with either DC-EVIR or DC-CtrlR that had been preincubated with EVs isolated from HER2$^+$ or negative MC38 cells expressing OVA (EV-HER2/OVA and EV-OVA, respectively). EV-HER2/OVA greatly enhanced the proliferation of CD8$^+$ OT-I cells cocultured with DC-EVIR cells, compared to the other conditions (**Fig. 1e** and **Supplementary Fig. 5a**,**b**). Of note, we did not observe T-cell proliferation in response to EV-HER2/OVA in the absence of DCs. T-cell proliferation induced by DC-EVIR plateaued at lower EV-HER2/OVA doses, compared to DC-CtrlR (**Supplementary Fig. 5c**). Thus, the anti-HER2 EVIR enhances

Swiss Institute for Experimental Cancer Research (ISREC), School of Life Sciences, École Polytechnique Fédérale de Lausanne (EPFL), Lausanne, Switzerland.
Correspondence should be addressed to M.D.P. (michele.depalma@epfl.ch) or M.L.S. (mario.squadrito@epfl.ch).

RECEIVED 27 MAY 2017; ACCEPTED 22 NOVEMBER 2017; PUBLISHED ONLINE 22 JANUARY 2018; DOI:10.1038/NMETH.4579

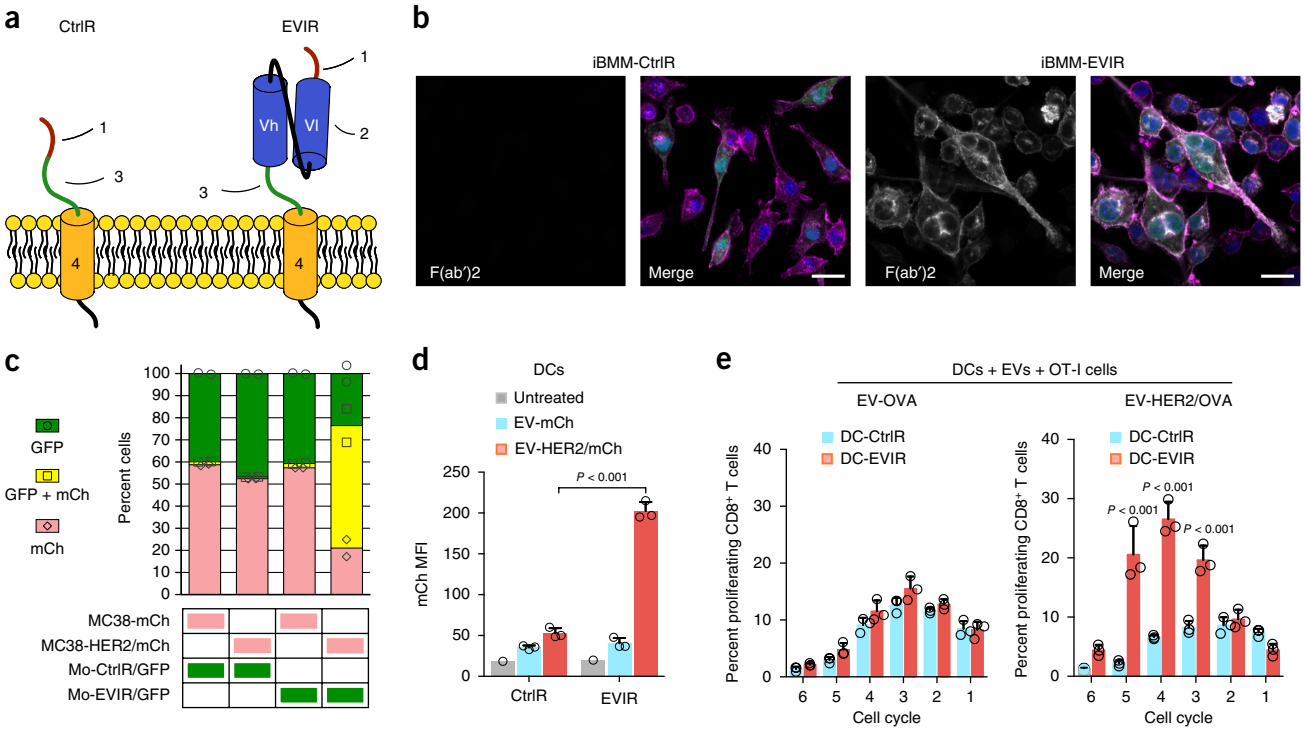

Figure 1 | An anti-HER2 EVIR promotes tumor EV uptake and antigen presentation by DCs. (**a**) Schematic representation of CtrlR (left) and EVIR (right) on the cell membrane. The extracellular domain comprises an IgK signal peptide (1), an scFv domain (2; only present in the EVIR), and a hinge domain (3). The hinge domain and the transmembrane–intracellular domain (4) are derived from a nonsignaling, truncated dLNGFR. (**b**) Representative confocal images showing anti-scFv immunostaining (white) and the merger of anti-scFv (white), direct GFP fluorescence (green), actin fibers stained with phalloidin (magenta), and nuclear staining with DAPI (blue), in iBMM-CtrlR and anti-HER2 iBMM-EVIR cells. See **Supplementary Figure 1b** for individual staining images. The cells were analyzed 7 d post-transduction. Scale bar, 50 µm. Data are representative of three independent cell cultures. (**c**) Cell-binding assay using Mo-EVIR/GFP (or control Mo-CtrlR/GFP) and MC38-HER2/mCh (or control MC38–mCh) cells at 1:1 ratio; the cells were incubated in suspension for 20 min. Data indicate the proportion of cells that appear either as single cells (green or pink, representing monocytes and MC38 cells, respectively) or in clusters (yellow, representing monocytes bound to MC38 cells), according to flow cytometry analysis. Two independent cell cultures per condition are shown. (**d**) Median fluorescence intensity (MFI) of mCh in DC-CtrlR and DC-EVIR either untreated or treated with EV-mCh or EV-HER2/mCh. Data indicate mean values ± s.e.m. (n = 3 independent cell cultures per condition); statistical analysis by two-way ANOVA with Sidak's multiple comparison test. (**e**) Flow cytometry analysis of CD8$^+$ OT-I proliferation, assessed by CellTrace dilution, after coculture with DC-CtrlR or DC-EVIR cells exposed to EV-OVA or EV-HER2/OVA. Data show the percentage (mean values ± SEM; n = 3 independent cell cultures per condition) of CD8$^+$ OT-I cells that have completed a defined number of cell cycles (1 to 6). Statistical analysis by two-way ANOVA with Sidak's multiple comparison test. Numerical values for the experiments with quantitative data are presented in **Supplementary Table 2**.

MHCI-mediated presentation of a surrogate TA contained in HER2-positive EVs.

Cross-dressing defines the DC's acquisition of MHCI–antigen complexes shed by other cells[12,13]. We asked whether the EVIR enhances TA presentation preferentially through classical TA internalization, processing and cross-presentation[14], or by promoting DC cross-dressing with EV-associated, preformed MHCI–antigen complexes. We deleted either the MHCI subunit *B2m*, which is common to all MHCI complexes, or *H2kb*, which is specific for the SIINFEKL peptide, in MC38-HER2/OVA and MC38-OVA cells using an LV-based CRISPR–Cas9 strategy (**Supplementary Fig. 6a**,**b**). Both *B2m* and *H2kb* knockout (KO) cells had an intact OVA transgene (**Supplementary Fig. 6c**) and released EVs that were comparable, according to abundance and size distribution, to those of unmodified cells (**Supplementary Fig. 6d**). Also, we did not observe differences between EVs isolated from cells deficient and proficient (unmodified) in *B2m* or *H2kb* when we analyzed EV internalization by DCs (**Supplementary Fig. 6e**).

Unexpectedly, DC-EVIR failed to promote CD8$^+$ OT-I proliferation in the presence of EVs isolated from either *H2kb or B2m* KO cancer cells (**Fig. 2a** and **Supplementary Fig. 7a**), which suggested that MHCI–antigen complexes carried by EVs are required to stimulate OVA-specific T-cell proliferation. To validate these results, we generated BMDCs from *B2m* KO mice[15] and found that the lack of endogenous MHCI–SIINFEKL complexes on the DCs (**Supplementary Fig. 7b**) did not prohibit EVIR-mediated enhancement of T-cell proliferation in the presence of EV-HER2/OVA (**Fig. 2b**). Mass-spectrometry analysis indicated that MC38-derived EVs contain H-2Kb (**Supplementary Table 1**), which supported a mechanism of horizontal transfer of H-2Kb from the EVs to the DCs.

In order to analyze EV-mediated H-2Kb transfer, we used DCs generated from FVB/n mice, which lack H-2Kb (**Supplementary Fig. 7c**). In this setting, EV-HER2/OVA transferred H-2Kb to H-2Kb$^-$ DCs in an EVIR-dependent manner (**Supplementary Fig. 7d**). Moreover, H-2Kb$^+$ MC38-HER2/GFP cells efficiently transferred H-2Kb to H-2Kb$^-$ DC-EVIR in a DC–cancer-cell comingling assay performed in immunodeficient NSG mice (**Supplementary Fig. 8a–d**), which also lack endogenous H-2Kb MHCI (**Supplementary Fig. 7c**). Collectively, these data indicate that the

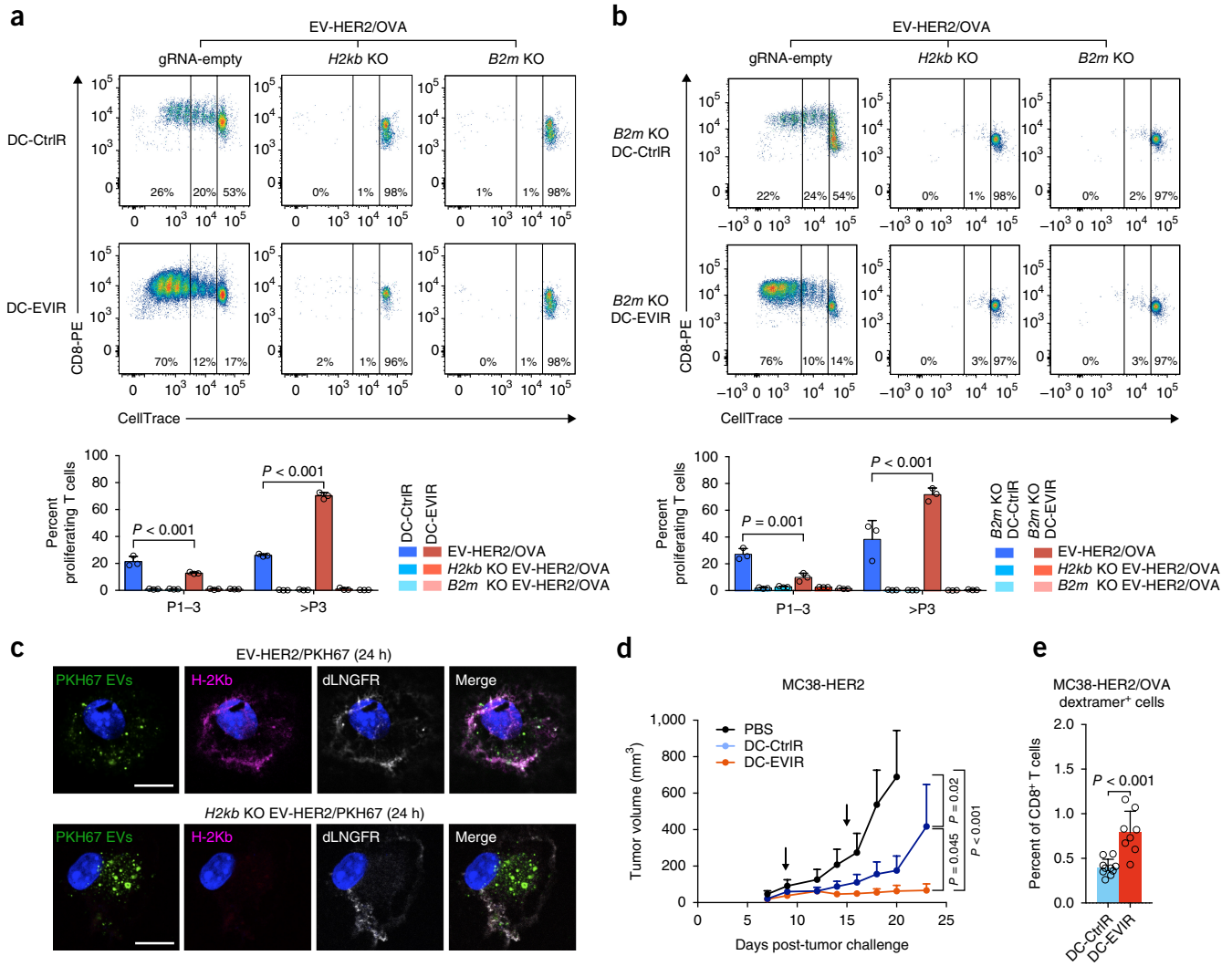

Figure 2 | An anti-HER2 EVIR cross-dresses DCs with EV-derived MHCI–antigen complexes and enhances the antitumoral capacity of DC vaccination in mice. (**a**,**b**) Flow cytometry analysis of CD8⁺ OT-I proliferation, assessed by CellTrace dilution, after coculture with DCs and EVs, as indicated. The top panels show representative flow cytometry dot plots. The bottom panels show the percentage of CD8⁺ OT-I cells that completed 1 to 3 (P1–3) or more than 3 (>P3) cell cycles. Data show mean percentage values ± s.e.m. (n = 3 independent cell cultures per condition); statistical analysis by two-way ANOVA with Tukey's multiple comparison test. (**c**) H-2Kb-negative DC-EVIR obtained from FVB/n mice were incubated with PKH67-labeled (green), *H2kb* wild-type (top panels), or KO (bottom panels) EV-HER2 and analyzed after 24 h. The cells were stained with antibodies to reveal H-2Kb (magenta) and dLNGFR (white). Nuclei were labeled with DAPI (blue). Scale bar, 10 µm. Images are representative of ten cells per condition; additional images are shown in **Supplementary Figure 11**. Data are representative of two independent cell culture experiments. (**d**) Volume of subcutaneous MC38-HER2 tumors in mice vaccinated with two sequential DC infusions, indicated by the arrows. Data show mean tumor volume ± s.e.m. (PBS, n = 4 mice; DC-CtrlR, n = 7; DC-EVIR, n = 9). Statistical analysis by two-way ANOVA with Tukey's multiple comparison test. The experiment was performed one time. (**e**) Flow cytometry analysis showing the percentage of OVA-specific (dextramer⁺) CD8⁺ T cells in the spleens of MC38-HER2/OVA tumor-bearing mice, vaccinated with DCs as indicated. Data show mean percentage values ± s.e.m. (DC-CtrlR, n = 10 mice; DC-EVIR, n = 8); statistical analysis by two-tailed unpaired Student's t-test. The experiment was performed one time. The gating strategy is presented in **Supplementary Figure 13**. Numerical values for the experiments with quantitative data are presented in **Supplementary Table 2**.

EVIR enables TA presentation largely by cross-dressing DCs with EV-derived MHCI–antigen complexes.

We then studied the mechanism of MHCI transfer to DCs. PKH67-labeled HER2⁺ EVs (EV-HER2/PKH67) were protected from trypsin and acid digestion as early as 2 h after incubation with DC-EVIR, which is indicative of rapid EV internalization (**Supplementary Fig. 9a**). Two micropinocytosis and phagocytosis inhibitors, amiloride and cytochalasin-D, blocked EV internalization, whereas an inhibitor of clathrin-mediated endocytosis had modest effects on EV internalization (**Supplementary Fig. 9b**). Accordingly, EV-HER2/PKH67 that had been internalized by DC-EVIR largely colocalized with fluorescently labeled dextran, which is internalized through a macropinocytosis-dependent endocytic pathway, but not with transferrin, which is internalized through receptor-dependent, clathrin-mediated endocytosis (**Supplementary Fig. 9c**). Of note, EV-HER2/PKH67 that had been internalized by DC-CtrlR did not specifically associate with dextran, suggesting that the EVIR enhanced EV internalization via macropinocytosis.

We then used EV-HER2/mCh to trace the fate of the EVs following internalization by DCs (**Supplementary Fig. 10a–d**).

As early as 1 h after EV incubation with DCs, the mCh signal colocalized with EEA1$^+$ early endosomes in both DC-EVIR and DC-CtrlR. At 5 h, mCh colocalized with both RAB11$^+$ recycling endosomes and LAMP1$^+$ lysosomes; however, DC-EVIR showed enhanced sorting to recycling endosomes and decreased sorting to lysosomes compared to DC-CtrlR. These results suggest that the EVIR encourages the shunting of EV cargo from degradation to recycling, a process that may account for EVIR-mediated MHCI cross-dressing. To extend these findings, we also analyzed the kinetics of H-2Kb internalization and recycling in H-2Kb$^-$ DC-EVIR that had been exposed to H-2Kb$^+$ EV-HER2/PKH67 (**Fig. 2c** and **Supplementary Fig. 11**). Most of the H-2Kb colocalized with internalized EVs at 5 h, consistent with the expected kinetics of EV endocytosis. However, H-2Kb colocalization with the plasma membrane became evident at 24 h. These results indicate that EVIR-engineered DCs can internalize and recycle functional MHCI–peptide complexes by adsorbing tumor-derived EVs.

To explore the versatility of the EVIR platform, we designed an EVIR specific for the disialoganglioside GD2, which is highly expressed in human melanoma[16]. In order to obtain GD2-expressing cancer cells, we transduced MC38–mCh cells with LVs encoding for the GD2 synthases GD2S and GD3S[17]. This resulted in robust GD2 expression by nonmelanoma MC38–mCh cells (**Supplementary Fig. 12a**). Expression of the anti-GD2 EVIR in iBMMs enhanced the ability of these iBMMs to acquire mCh fluorescence from EVs isolated from GD2$^+$ MC38–mCh cells (**Supplementary Fig. 12b**).

We also examined CD8$^+$ OT-I proliferation in response to GD2$^+$ melanoma-derived EVs and anti-GD2 EVIR-transduced DCs. For these experiments, we engineered the OVA-positive mouse melanoma cell line SM1-OVA to express GD2 (**Supplementary Fig. 12c**). Because cross-dressing requires MHCI expression in the cancer cells, we stimulated MHCI expression in SM1-OVA cells with interferon-γ (IFNγ; **Supplementary Fig. 12d**). We then cocultured CD8$^+$ OT-I cells with either DC-EVIR or DC-CtrlR, and we treated the coculture with EVs isolated from either IFNγ-stimulated or unstimulated SM1-GD2/OVA cells (EV-SM1-GD2/OVA^{IFN} and EV-SM1-GD2/OVA, respectively; **Supplementary Fig. 12e**). In the presence of EV-SM1-GD2/OVA^{IFN}, the DC-EVIR cells enhanced CD8$^+$ OT-I proliferation compared to DC-CtrlR (**Supplementary Fig. 12f**). Conversely, EV-SM1-GD2 did not stimulate OT-I proliferation, likely because of the low amounts of MHCI–peptide complexes on the surface of these EVs. These results provide further evidence that EVIRs can be broadly used to stimulate TA-specific responses through DC cross-dressing.

To determine whether DC-EVIR can potentiate an antigen-specific antitumoral immune response, we inoculated MC38-HER2 cells subcutaneously in syngenic mice and, when the tumors were established, vaccinated the mice with either anti-HER2 DC-EVIR or DC-CtrlR cells. Vaccination with DC-EVIR inhibited MC38-HER2 tumor growth more efficiently than vaccination with DC-CtrlR (**Fig. 2d**). In an independent experiment that used MC38-HER2/OVA cells, we observed a small but statistically significant expansion of endogenous, tumor-specific CD8$^+$ T cells in the spleen of mice that had been vaccinated with DC-EVIR, compared to DC-CtrlR (**Fig. 2e** and **Supplementary Fig. 13**). These data suggest that EVIR-engineered DCs can promote antitumoral responses by harnessing tumor-derived EVs and their cargo of TAs.

In future applications, the EVIR platform may be exploited for identifying EV-associated TAs and cognate T-cell receptors (TCRs) through *ex vivo* cell assays, or for enhancing the priming of CD8$^+$ T cells toward unknown, patient- and tumor-specific TAs in therapeutic DC vaccination settings. DC-EVIR vaccination may be combined with strategies that enhance T-cell activation and alleviate cancer-associated immunosuppression through, for example, vascular reprogramming, macrophage depletion, or immune checkpoint blockade[18,19].

METHODS

Methods, including statements of data availability and any associated accession codes and references, are available in the online version of the paper.

Note: Any Supplementary Information and Source Data files are available in the online version of the paper.

ACKNOWLEDGMENTS

We are grateful to G. Guarda (University of Lausanne, UNIL, Switzerland) for providing BM cells of *B2m*-deficient mice; N. Haynes (Peter MacCallum Cancer Center, Melbourne, Australia) for MC38-OVA cells; A. Ribas (University of California, Los Angeles, California, USA) for SM1-OVA cells; A. Donda, J. Mach, and D. Speiser (UNIL) for valuable scientific advice; A. Lombardo (Vita-Salute San Raffaele University, Milan, Italy) for advice with CRISPR LVs; A. Royant (Institut de Biologie Structurale, Grenoble, France) for providing the mTq sequence; L. Trusolino (University of Torino Medical School, Italy) for providing the *HER2* sequence; D. Thompson and L. Giesbrecht for technical help; and the EPFL core facilities of flow cytometry (FCCF), proteomics (PCF), and bioimaging/optics platform (BIOp), for skillful assistance. S.K.H. was supported by the Swiss Federal Commission for Scholarships for Foreign Students (Swiss Government Excellence Scholarship 2015.0430). This study was funded by grants from the European Research Council (ERC-CoG EVOLVE 725051), the EPFL Catalyze4Life program, and the Swiss National Foundation (SNF grant 31003A-165963) to M.D.P.

AUTHOR CONTRIBUTIONS

M.L.S. constructed LVs, designed and performed research, analyzed and interpreted the data, assembled the display items, and wrote the manuscript. C.C. designed and analyzed EV internalization and MHCI recycling assays and contributed to the writing of the manuscript. S.K.H. performed some experiments. M.D.P. designed and supervised research, interpreted the data, and wrote the manuscript.

COMPETING FINANCIAL INTERESTS

The authors declare competing financial interests: details are available in the online version of the paper.

1. Simons, M. & Raposo, G. *Curr. Opin. Cell Biol.* **21**, 575–581 (2009).
2. Tkach, M. & Théry, C. *Cell* **164**, 1226–1232 (2016).
3. Becker, A. *et al. Cancer Cell* **30**, 836–848 (2016).
4. Bobrie, A. & Théry, C. *Biochem. Soc. Trans.* **41**, 263–267 (2013).
5. Wolfers, J. *et al. Nat. Med.* **7**, 297–303 (2001).
6. Zhang, B., Yin, Y., Lai, R.C. & Lim, S.K. *Front. Immunol.* **5**, 518 (2014).
7. Gu, X., Erb, U., Buchler, M.W. & Zöller, M. *Int. J. Cancer* **136**, E74–E84 (2015).
8. Arteaga, C.L. *et al. Nat. Rev. Clin. Oncol.* **9**, 16–32 (2011).
9. Amendola, M., Venneri, M.A., Biffi, A., Vigna, E. & Naldini, L. *Nat. Biotechnol.* **23**, 108–116 (2005).
10. Squadrito, M.L. *et al. Cell Rep.* **8**, 1432–1446 (2014).
11. Hogquist, K.A. *et al. Cell* **76**, 17–27 (1994).
12. Dolan, B.P., Gibbs, K.D. Jr. & Ostrand-Rosenberg, S. *J. Immunology* **177**, 6018–6024 (2006).
13. Wakim, L.M. & Bevan, M.J. *Nature* **471**, 629–632 (2011).
14. Joffre, O.P., Segura, E., Savina, A. & Amigorena, S. *Nat. Rev. Immunol.* **12**, 557–569 (2012).
15. Ludigs, K. *et al. Nat. Commun.* **7**, 10554 (2016).
16. Ahmed, M. & Cheung, N.K. *FEBS Lett.* **588**, 288–297 (2014).
17. Groux-Degroote, S., Guérardel, Y. & Delannoy, P. *Chembiochem* **18**, 1146–1154 (2017).
18. Baer, C. *et al. Nat. Cell Biol.* **18**, 790–802 (2016).
19. Palucka, A.K. & Coussens, L.M. *Cell* **164**, 1233–1247 (2016).

ONLINE METHODS

Design and construction of lentiviral vectors encoding EVIRs. In order to generate an anti-HER2 EVIR, a mouse-optimized DNA sequence coding for the CHA21 scFv, designed according to a previous study[20], was obtained from GeneArt (Life Technologies). A DNA sequence coding for the IgK signal peptide (MDFQVQIFSFLLISASVIMSRG) was incorporated at the 5′-end of the CHA21 sequence to enable the export of the receptor to the cell membrane. A DNA sequence containing a high-efficiency Kozak sequence and a BamHI restriction site was incorporated at the 5′-end of the CHA21-IgK DNA sequence. We also inserted a DNA sequence containing AgeI, MluI, and XhoI restriction sites, and a stop codon (TGA), at the 3′-end of the CHA21-IgK coding sequence.

The synthetic DNA sequence encoding the IgK-CHA21 construct was then inserted in a LV plasmid downstream to a spleen forming focus virus (SFFV) promoter and upstream to the WPRE-stabilizing sequence[21] by using the BamHI and SalI restriction sites of the plasmid.

A human truncated low-affinity nerve growth factor receptor (dLNGFR), comprising the intracellular (IC) domain, the transmembrane (TM) domain, and a segment of the extracellular (EC) domain, was obtained by polymerase chain reaction (PCR) from a plasmid containing a dLNGFR sequence[21] using the following primers containing AgeI and MluI restriction sites:

Fw (AgeI): AAAAAACCGGTCTTCTGGGGGTGTCCCTTG
Rv (Mlu): AAAAAACGCGTAGTTAGCCTCCCCCATCTCC

The PCR product was then cloned using AgeI and MluI restriction sites downstream to the CHA21 sequence and upstream to the stop codon in the SFFV.IgK-CHA21.WPRE plasmid, producing the SFFV.EVIR.WPRE LV.

In order to enable tracing of EVIR expression, the SFFV.EVIR.WPRE sequence was cloned into a bidirectional LV[9] by replacing the human PGK (hPGK).dLNGFR cassette with the SFFV.EVIR cassette using EcoRV and AvrII restriction sites. In this bidirectional LV, the GFP is expressed under the transcriptional control of the minimal cytomegalovirus promoter (mCMV). The full amino acid sequence of the anti-HER2 EVIR is as follows:

>anti-HER2_EVIR

MDFQVQIFSFLLISASVIMSRGDIVLTQTPSSLPVSVGEKV
TMTCKSSQTLLYSNNQKNYLAWYQQKPGQSPKLLISWAFT
RKSGVPDRFTGSGSGTDFTLTIGSVKAEDLAVYYCQQYSN
YPWTFGGGTRLEIKRGGGGSGGGGSGGGGSGGGGSEVQ
LQQSGPEVVKTGASVKISCKASGYSFTGYFINWVKKNSGK
SPEWIGHISSSYATSTYNQKFKNKAAFTVDTSSSTAFMQLN
SLTSEDSAVYYCVRSGNYEEYAMDYWGQGTSVTVSSTGLL
GVSLGGAKEACPTGLYTHSGECCKACNLGEGVAQPCGAN
QTVCEPCLDSVTFSDVVSATEPCKPCTECVGLQSMSAPCV
EADDAVCRCAYGYYQDETTGRCEACRVCEAGSGLVFSCQD
KQNTVCEECPDGTYSDEANHVDPCLPCTVCEDTERQLRE
CTRWADAECEEIPGRWITRSTPPEGSDSTAPSTQEPEAPPEQ
DLIASTVAGVVTTVMGSSQPVVTRGTTDNLIPVYCSILAAV
VVGLVAYIAFKRWNRGIL

In order to generate an anti-GD2 EVIR, a mouse-optimized anti-GD2 14.G2a scFv sequence, designed according to a previous study[22], was obtained from GeneArt. Construction of this EVIR used molecular cloning steps that were analogous to those used for constructing the anti-HER EVIR. Briefly, a sequence coding for the IgK signal peptide (described above) was cloned at the 5′-end of the 14.G2a sequence. A DNA sequence containing a high-efficiency Kozak sequence and a BamHI restriction site was incorporated at the 5′-end of the 14.G2a scFv coding sequence, as described above. A restriction site for AgeI was incorporated at the 3′-end of the scFv. The CHA21-IgK sequence in the SFFV.EVIR.WPRE LV was then replaced with the 14G.2a-IgK sequence. The resulting SFFV.EVIR.WPRE sequence was cloned into the bidirectional LV described above. The full amino acid sequence of the anti-GD2 EVIR is as follows:

>anti-GD2_EVIR

MDFQVQIFSFLLISASVIMSRGEVQLLQSGPELEKPGASVM
ISCKASGSSFTGYNMNWVRQNIGKSLEWIGAIDPYYGGTSY
NQKFKGRATLTVDKSSSTAYMHLKSLTSEDSAVYYCVSGMEY
WGQGTSVTVSSGGGGSGGGGSGGGGSDVVMTQTPLSLPVS
LGDQASISCRSSQSLVHRNGNTYLHWYLQKPGQSPKLLIHK
VSNRFSGVPDRFSGSGSGTDFTLKISRVEAEDLGVYFCSQSTH
VPPLTFGAGTKLELTGLLGVSLGGAKEACPTGLYTHSGECCK
ACNLGEGVAQPCGANQTVCEPCLDSVTFSDVVSATEPCKPC
TECVGLQSMSAPCVEADDAVCRCAYGYYQDETTGRCEACR
VCEAGSGLVFSCQDKQNTVCEECPDGTYSDEANHVDPCLP
CTVCEDTERQLRECTRWADAECEEIPGRWITRSTPPEGSDST
APSTQEPEAPPEQDLIASTVAGVVTTVMGSSQPVVTRGTTD
NLIPVYCSILAAVVVGLVAYIAFKRWNRGIL

The CtrlR-expressing LV was obtained by cloning the dLNGFR sequence without the scFv sequence in the SFFV.WPRE LV using BamHI and SalI restriction enzymes. The resulting SFFV.CtrlR.WPRE sequence was then cloned in the bidirectional LV described above.

Construction of lentiviral vectors encoding other transgenes. In order to express mTurquoise2 (mTq), we generated a CMV.mTq.WPRE LV by replacing the GFP sequence in the CMV.GFP.WPRE LV, described previously[21], with the mTq coding sequence[23] (a gift of A. Royant, Institut de Biologie Structurale, Grenoble, France), using BamHI and SalI restriction sites.

In order to express HER2 in cancer cells, we generated an hPGK.HER2.WPRE LV by replacing the mCherry (mCh) coding sequence in the hPGK.mCh.WPRE LV, described previously[10], with a human HER2 coding sequence[24] provided by L. Trusolino (University of Torino Medical School, Italy), using BamHI and SalI restriction sites.

In order to express GD2 in cancer cells, we generated two LVs, hPGK.GD2S.WPRE and hPGK.GD3S.WPRE, by replacing the *HER2* coding sequence in the LV described above with mouse-optimized sequences encoding GD2 synthase (NCBI accession: NM_027739) or GD3 synthase (NCBI accession: NM_011374), respectively, obtained from GeneArt, using BamHI and SalI restriction sites.

In order to disrupt *H2kb* or *B2m* in MC38 cells, we generated self-inducible CRISPR–Cas9-based LVs. We obtained an LV containing both a TetO-CAS9 expression cassette and an hPGK promoter-regulated bicistronic cassette for the expression of the reverse tTA (rtTA) and puromycin (PURO) (a gift of A. Lombardo, San Raffaele Scientific Institute, Milan, Italy). We then obtained from GeneArt a DNA sequence containing a U6-driven gRNA hosting a BsmBI cloning site for rapid and one-step annealing and ligation of crRNA sequences against the gene of interest. We cloned the U6-gRNA cassette upstream to the TetO-CAS9 expression cassette using ClaI and XhoI restriction sites to obtain

the doxycycline-self-inducible U6-sgRNA.TetO-CAS9.hPGK-PURO/2A/rtTA LV (shown in **Supplementary Fig. 6a**). In order to employ the ClaI restriction site, the U6-sgRNA.TetO-CAS9.hPGK-PURO/2A/rtTA plasmid was expanded and isolated in the *dam*-deficient *E. coli* strain GM2163. We then sought to remove BsmBI restriction sites interfering with the process of one-step cloning. To this aim, we replaced the hPGK and PURO sequences in the parental plasmid with mutated hPGK and PURO sequences obtained from GeneArt. Both mutated sequences were cloned in the U6-sgRNA.TetO-CAS9.hPGK-PURO/2A/rtTA LV using BamHI and XbaI restriction sites. We then annealed and ligated the DNA oligos shown below using the BsmBI restriction site of the U6-sgRNA.TetO-CAS9.hPGK-PURO/2A/rtTA LV.

gRNA sequences:
Control gRNA: GCGAGACGACCATGGACGTCTCC
H2kb gRNA: GGGCCCGGTACTCACCCGCG
B2m gRNA: GGTCGTCAGCATGGCTCGCT
Oligos to generate genome-targeting gRNAs:
gR_*H2k1*_1_Se: ACCGGGCCCGGTACTCACCCGCG
gR_*H2k1*_1_AS: AAACCGCGGGTGAGTACCGGGCC
gR_*B2m*_1_Se: ACCGGTCGTCAGCATGGCTCGCT
gR_*B2m*_1_AS: AAACAGCGAGCCATGCTGACGAC

Cell lines and primary cell cultures. Immortalized murine-bone-marrow-derived macrophages (iBMM) were described previously[10]. iBMMs were cultured in Iscove's Modified Dulbecco's Medium (IMDM, Sigma) supplemented with mouse colony-stimulating factor-1 (CSF1, 50 ng/ml, Peprotech), L-glutamine and penicillin–streptomycin (Life Technologies), and 20% fetal bovine serum (FBS; EuroClone Group).

Murine P388D1 monocytic cells, MC38 and MC38-OVA colon carcinoma cells (provided by N. Haynes, Peter MacCallum Cancer Center, Melbourne), SM1-OVA melanoma cells (provided by A. Ribas, University of California, Los Angeles, California), and human 293T embryonic kidney cells, were cultured in IMDM supplemented with 10% FBS, glutamine, and penicillin–streptomycin. In some experiments, SM1-OVA cells were stimulated with interferon-γ (IFNγ; Peprotech) for 24 h before use.

Bone marrow (BM) cells were obtained by flashing femurs and tibiae of 6–8-week-old wild-type (C57Bl/6 or FVB/n) or *B2m* KO (C57Bl/6) mice[25] with ice-cold PBS. BM cells of *B2m*-deficient mice were a gift of G. Guarda (University of Lausanne, Switzerland). In order to generate dendritic cells (DCs), BM cells were cultured for 7–8 d in RPMI medium supplemented with GM-CSF (100 ng/ml, Peprotech) and IL4 (40 ng/ml, Peprotech), 10% FBS, glutamine, and penicillin–streptomycin.

Lentiviral vector production. Vesicular stomatitis virus (VSV)-pseudotyped, third-generation LVs were produced by transient five-plasmid cotransfection into 293T cells, as described previously[26], with some modifications. Briefly, 9 million 293T cells were seeded in 15 cm dishes 24 h before transient transfection in 20 ml of cell culture medium. For each dish, a plasmid mix was prepared containing (i) the envelope plasmid (VSV-G, 9 μg), (ii) the packaging pMDLg/pRRE plasmid (12.5 μg), (iii) the REV plasmid (6.25 μg), (iv) the pADVANTAGE plasmid (15 μg), and (v) the transfer lentiviral plasmid (32 μg). Transient transfection was performed as previously described[26]. After 30 h, the cell supernatant was collected, filtered (0.22 μm), and concentrated by ultracentrifugation using a Beckman ultracentrifuge equipped with a SW32Ti rotor, at 82,600 RCF for 2 h at 20 °C. LV particles were collected in PBS and stored at −80 °C.

LVs were titered using 293T cells. The percentage of marker (dLNGFR, HER2, GFP, mCh, or mTq)-positive cells was measured by flow cytometry 4–7 d after transduction, and the titer was calculated as previously described[26]. The titers of LVs used to express GD2S, GD3S, and the CRISPR–Cas9-based system were calculated by measuring the copy number of vector integrated per genome by quantitative PCR, as previously described[26]. We obtained titers ranging from 10^9 to 10^{10} transducing units (TU)/ml after LV ultracentrifugation.

Cell transduction. Stable cell line (MC38, MC38-OVA, SM1-OVA, P388D1, and iBMM) cells were transduced with LV doses ranging from multiplicity of infection (MOI) 5 to 10. In experiments with double transduction, the cells were transduced sequentially, 1 d apart. Transduced cells were propagated for several days or weeks and stored at −80 °C.

To transduce primary BM-derived DCs, BM cells were transduced with an LV dose of 100 MOI 2 d after seeding in RPMI supplemented with GM-CSF and IL4. 24 h post-transduction, transduced BM cells were washed and seeded for DC differentiation in the presence of GM-CSF and IL4 for at least 5–6 d before use.

Cell-binding assays. We performed cell-binding assays in cell-suspension conditions. Transduced P388D1 monocytes (Mo-EVIR and Mo-CtrlR) were incubated with MC38-HER2/mCh (or control MC38-mCh) cancer cells as follows. MC38 cells were detached by trypsin/EDTA, whereas P388D1 cells were detached by pipetting. After washing in PBS, MC38 and P388D1 cells were coincubated at either 1:1, 9:1, or 1:9 ratio in 100 μl of PBS at a concentration of 10^7 cells/ml at 4 °C in a spinning wheel for 20 min. Cells were immediately analyzed by flow cytometry or confocal microscopy (see below).

We performed cell-binding assays in cell adhesion conditions. We seeded 2×10^4 MC38-HER2/mTq (or control MC38-mTq) cancer cells in 24-well plates (Corning). 1 h later, we seeded iBMM-EVIR, iBMM-CtrlR, or iBMM-mCh cells on the cancer cells, at 1:1 ratio. After 24 h of coculture, cells were detached by a short incubation with trypsin/EDTA (3 min at 37 °C), washed with wash solution (PBS, 4 mM EDTA and 1% FBS), resuspended in wash solution containing 7-aminoactinomycin-D (7AAD, Sigma) to exclude dead cells, and immediately analyzed by flow cytometry (see below).

EV isolation, quantification, and labeling with PKH67. In order to isolate EVs, MC38, MC38-OVA, or SM1-OVA cells were cultured for at least 3 d in RPMI medium supplemented with FBS depleted of EVs by ultracentrifugation at 134,000 RCF for 6 h. The cell culture medium was centrifuged at 500 RCF for 5 min; 2,000 RCF for 5 min; and finally at 4,600 RCF for 20 min at 4 °C to remove cells and debris. The resulting medium was then ultracentrifuged at 134,000 RCF for 70 min at 4 °C using a Beckman ultracentrifuge and a SW32Ti rotor. EVs were resuspended in PBS and stored at −80 °C.

The size and concentration of the EV particles were determined by nanoparticle tracking analysis (NTA) using a Nanosight

doi:10.1038/nmeth.4579

NS300 device (Malvern Instruments, UK). Typically, purified EVs were diluted 1:100 or 1:1,000 in PBS before analysis. Three measurements of 60 s each were recorded for each sample.

EV labeling with PKH67 was performed by modifying the manufacturer's protocol (Sigma). Briefly, the EV preparations were diluted in diluent C before addition of PKH67 (1 µl per 100 µl of solution). Labeling was performed for 10 min at room temperature in the dark and terminated using 0.5% BSA (Sigma). EVs were washed twice with PBS and concentrated by ultracentrifugation as described above. The pellet was resuspended in PBS and stored at −80 °C. As a negative control for immunofluorescence studies, we diluted PKH67 in PBS and processed it by ultracentrifugation as described above.

Liquid chromatography-tandem mass spectrometry of EVs. EVs (10 µg of total protein, quantified by BCA protein assay kit; Thermo Fisher) were obtained from MC38 cells, as described above. The sample was processed as previously described[27]. Peptides were desalted using StageTips and dried in a vacuum concentrator. For LC-MS/MS analysis, the peptides were separated by reverse phase chromatography on a Dionex Ultimate 3000 RSLC nano UPLC system connected inline with an Orbitrap Elite (Thermo Fisher Scientific). Database search was performed using Mascot 2.5 (Matrix Science) and SEQUEST in Proteome Discoverer v.1.4. against a murine Uniprot protein database. Data were further processed and inspected in ScaffoldTM 4.8.4 (Proteome Software). Two independent analyses were performed on one EV preparation.

Immunofluorescence analysis of transduced iBMMs. iBMMs were seeded on 8-well glass chamber slides (Corning) coated with fibronectin (200 µg/ml, Peprotech) at a concentration of 2×10^4 cells/well. To visualize the EVIR, the cells were stained with a directly conjugated anti-F(ab′)2 antibody (see **Supplementary Table 3** for details) and phalloidin-AlexaFluor-546 (Life technologies), in the absence of blocking solution, followed by DAPI staining. After staining, the cells were washed, fixed, and processed for confocal microscopy as described below.

Immunofluorescence analysis of EV-treated DCs. BM-derived DCs were seeded on 8 mm round glass coverslips coated with poly-D-lysine (50 µg/ml, Sigma) in 48-well plates (Corning) at a concentration of about 1.25×10^5 cells/ml. The cells were incubated with EVs either containing mCh or pre-labeled with PKH67 (2×10^8 EVs/well according to NTA analysis, unless indicated otherwise) for the time specified in the figure legends. After cell incubation with the EVs, the cells were washed, fixed, and processed for confocal microscopy as described below.

DC treatment with tracers or inhibitors of endocytosis. In order to trace macropinocytosis and clathrin-mediated endocytosis, 70 kD TRITC-conjugated dextran (Sigma) or AlexaFluor-555-conjugated transferrin (Life Technologies) were respectively added (both at 30 µg/ml) to the DCs 5 min before incubation with PKH67-labeled EVs. After 2 h, the DCs were fixed and analyzed by immunofluorescence staining as described below.

In order to inhibit endocytosis, the DCs were treated with 1 µM cytochalasin-D (Sigma), 10 µM chlorpromazine (Sigma), or 150 µM 5-(N-Ethyl-N-isopropyl) amiloride (Sigma), which are nonspecific inhibitors of phagocytosis/macropinocytosis, chlatrin-mediated endocytosis (CME), and macropinocytosis, respectively, for 30 min before incubation with PKH67-labeled EVs. After 2 h, the DCs were fixed and analyzed by immunofluorescence staining as described below.

Preparation of iBMMs and DCs for confocal microscopy. At the end of the experiments, the cells were fixed in 4% in paraformaldehyde (PFA) for 15 min at room temperature in the dark. After removing the PFA, the cells were incubated for 30 min in blocking solution containing 0.3% Triton, 10% normal goat serum (NGS), and an anti-CD16/CD32 Fc receptor-blocking antibody (Fc block; see **Supplementary Table 3** for details) in PBS. Following immunofluorescence staining (see below), the slides were washed with PBS and stained with 4′,6-diamidino-2-phenylindole (DAPI, 1 µg/ml; Sigma) to reveal cell nuclei. The glass coverslips were mounted in Dako mounting medium (Agilent), dried overnight at room temperature, and analyzed by a confocal microscope.

Immunofluorescence staining of endosomal proteins. In order to visualize endosomal proteins, a staining solution was prepared by diluting the primary antibodies (anti-EEA1, anti-RAB11, or anti-LAMP1, along with directly-conjugated anti-LNGFR; see **Supplementary Table 3** for details) in blocking solution. The staining solution was added (120 µl per well) for an overnight incubation at 4 °C. After washing, secondary antibodies (see **Supplementary Table 3** for details) were added for 30 min in PBS containing 0.3% Triton. In all immunofluorescence imaging experiments, mCh was detected using a chicken anti-mCh primary antibody followed by AlexaFluor-555-conjugated anti-chicken secondary antibody.

Immunofluorescence staining of intracellular H-2Kb. For intracellular H-2Kb staining and confocal imaging, we used a modified protocol. Live cells were washed in blocking solution and then fixed with Fix/Perm solution (using the FOXP3 staining kit for flow cytometry; eBioscience) for 20 min on ice. After washes with PBS, the cells were incubated with a PE-conjugated anti-H-2Kb antibody for 30 min, washed extensively, fixed with 4% PFA, and processed for further staining as described above.

Image analysis after confocal microscopy. After data acquisition using a confocal microscope (Zeiss LSM 700), the images were processed and analyzed with ImageJ (NIH). Transduced cells were identified by the presence of membrane-associated dLNGFR.

The intracellular localization of the mCh signal was analyzed by quantifying the amount of mCh signal showing: (i) a punctate pattern associated to the plasma membrane; (ii) a punctate pattern inside the cell; or (iii) an intracellular diffuse pattern. Analysis of EV internalization was performed by measuring the area occupied by the PKH67 signal over the total cell area, defined by the dLNGFR membrane signal, and then expressed as percentage values. Colocalization analyses were performed by measuring the Manders' coefficient[28] with the ImageJ plugin JaCoP, reporting the fraction of mCh^+ or $PKH67^+$ area overlapping with the selected endocytosis marker/tracer-positive area.

Flow cytometry. Flow cytometry used an LSR2 device (BD Bioscience); in all experiments, the fluorescence of GFP, mTq, and mCh was directly detected using the 488-525/50, 450-450/50, and

561-610/20 channels, respectively. The full list of primary antibodies used for flow cytometry is reported in **Supplementary Table 3**.

Flow cytometry of iBMM and DC cultures. After cell culture, iBMMs were detached with trypsin/EDTA, whereas DCs were detached by pipetting. For dLNGFR and B2M analysis, the cells were stained with directly conjugated primary antibodies (see **Supplementary Table 3** for details) in the presence of blocking solution. For F(ab)2 analysis, the cells were stained with a directly conjugated anti-F(ab)2 antibody (see **Supplementary Table 3** for details) without other antibodies. The cells were finally resuspended in 7AAD-containing wash solution to exclude dead cells.

For EV treatment studies, iBMMs were seeded in 24-well plates (10^5/well) and DCs in 96-well plates (2×10^4/well). Cells were incubated with 2×10^8 EVs/well (according to NTA analysis), except where indicated otherwise. iBMMs were detached with trypsin/EDTA, whereas DCs were detached by pipetting; the cells were then washed with a mild acid solution (50 mM acetic acid, Sigma) to remove EVs attached to the cell membrane. Before flow cytometry analysis of PKH67, mCh, or mTq fluorescence, the cells were stained with an APC-conjugated anti-dLNGFR antibody in the presence of Fc block. For H-2Kb staining, the cells were incubated with PE-conjugated anti-H-2Kb and APC-conjugated anti-dLNGFR antibodies, in the presence of Fc block (see **Supplementary Table 3** for details). The cells were finally resuspended in 7AAD-containing wash solution to exclude dead cells.

Flow cytometry of cancer cell lines. After cell culture, cancer cells were detached with trypsin/EDTA. For B2M, H-2Kb, HER2, and GD2 staining, the cells were stained with directly conjugated primary antibodies (see **Supplementary Table 3** for details) in the presence of Fc block. Before analysis, the cells were resuspended in 7AAD-containing wash solution.

Flow cytometry of EVs. To analyze HER2 on EVs, we stained 10^9–10^{10} EVs in 100 µl of PBS containing an AlexaFluor-647-conjugated anti-HER2 antibody in the presence of Fc block. After 15 min at 4 °C, the preparations were washed and the EVs isolated by ultracentrifugation as described above. EVs were resuspended in PBS and analyzed using an LSR2 device (BD Bioscience).

Isolation of CD8$^+$ OT-I cells. CD8$^+$ OT-I cells were isolated from OT-I TCR transgenic mice, which produce MHC class I-restricted, ovalbumin (OVA)-specific CD8$^+$ T cells[11]. The spleens were collected under sterile conditions, smashed and filtered by using gravity-driven 70 µm cell strainers to obtain single-cell suspensions. We depleted CD11c$^+$ cells with anti-CD11c microbeads (Miltenyi Biotech) and an autoMACS Pro separator apparatus. Subsequently, we positively selected CD8$^+$ T cells using anti-CD8 microbeads (Miltenyi Biotech). CD8$^+$ T cells were maintained in RPMI medium complemented with FBS, L-glutamine and penicillin–streptomycin, nonessential amino acid solution (Sigma), sodium pyruvate (1 mM, Gibco), and 2-mercaptoethanol (25 µM, Gibco).

OT-I proliferation assays. CD8$^+$ OT-I cells were stained with CellTrace-violet (Life Technologies) following the manufacturer's instructions. One-2×10^5 CD8$^+$ OT-I cells were cocultured in flat-bottom 96-well plates with $1–2 \times 10^4$ DCs. In the experiment shown in **Figure 1e**, DCs were preincubated for 24 h with EV-HER2/OVA (or control EV-OVA), washed extensively with PBS, and then added to the OT-I cells (day 0). In other experiments, DCs and T cells were incubated with EVs concomitantly (day 0). Unless indicated otherwise, 10^8–10^9 EV particles were employed in each cell culture. In all experiments, the proliferation of CD8$^+$ OT-I cells was measured at day 3 by flow cytometry by gating and analyzing CD8$^+$7AAD$^-$ T cells.

Generation of B2m and H2kb knockout MC38 cells. MC38, MC38-OVA, and MC38-HER2/OVA cells were transduced with CRISPR–CAS9 LVs expressing gRNA targeting either *B2m* or *H2kb*. 48 h after transduction, the cells were cultured in IMDM medium complemented with FBS, L-glutamine, penicillin–streptomycin, puromycin (10 µg/ml, Sigma) and doxycycline (10 µg/ml, Sigma) for 4 d. The cells were then plated at a concentration of 0.5 cell/well in 96-well plates in normal cell culture medium to isolate cell clones. Cell colonies showing no expression of B2M or H-2Kb by flow cytometry were expanded and employed in experiments.

OVA DNA analysis. Genomic DNA was extracted from MC38 cells either untransduced or transduced with the CRISPR–CAS9 LVs, using the DNeasy Blood & Tissue Kit (Qiagen). OVA sequences were amplified by PCR using the following primers:

OVA_Fw: TTGCCAGTGGGACAATGAGC
OVA_Rv: GTTGGTTGCGATGTGCTTGAT

Mouse studies. Mice employed in this study were maintained in a pathogen-free barrier animal facility according to the Swiss regulations for animal care and experimental research. OT-I TCR transgenic mice were available at EPFL. C57Bl6/J, FVB/n, and Nod SCID gamma (NSG) mice were purchased from Charles River Laboratory (L'Arbresle, France). All procedures were approved by the Veterinary Authorities of the Canton Vaud according to the Swiss law (protocols 3154 and 2916).

DC vaccination of tumor-bearing mice. MC38-HER2 and MC38-HER2/OVA tumors were generated by injection of 1×10^6 cells subcutaneously into the right flank of 6-week-old C57Bl6/J mice. In both experiments, DC vaccinations were performed at day 7 and 14 post-tumor challenge via peritumoral injection of 10^6 DCs in 100 µl of PBS (or PBS alone as control). The volume of MC38-HER2 tumors was determined by caliper measurements and calculated using the formula: volume = $\pi/6 \times d \times D^2$, where d is the shorter and D the longer tumor axis. MC38-HER2/OVA tumors regressed spontaneously after a short-lived growth phase, so tumor volume data could not be considered reliable.

Analysis of OVA-specific T cells in tumor-bearing mice. To analyze OVA-specific T cells in MC38-HER2/OVA tumor-bearing mice, the mice were euthanized at day 19 post-tumor injection. After isolation and processing of the spleen (see above), single-cell suspensions were stained for 30 min with OVA-specific MHCI dextramer-APC (Immudex) diluted at 1:2 and subsequently stained with lineage-specific conjugated antibodies for 15 min at 4 °C. The CD8$^+$ OT-I cells were identified as dextramer$^+$CD45$^+$CD11b$^-$ CD4$^-$CD8$^+$7AAD$^-$ cells.

doi:10.1038/nmeth.4579

Tumor–DC comingling assay. Transduced DCs (10^6 cells) of FVB/n origin (H-2Kb-negative) were embedded in 200 µl of matrigel (BD Bioscience) together with *H2kb* wild-type or knockout MC38-HER2/OVA cells (10^6 cells). The matrigel was supplemented with 0.5 µg of bFGF, 0.5 µg of GM-CSF (both from Peprotech) and 0.25 µg of sphingosine-1-phosphate (Cayman Chemical). Matrigel plugs containing cancer cells and DCs were then implanted subcutaneously in the flank of 8-week-old female NSG mice, which do not express H-2Kb; the matrigel implant sustains the growth of tumor-forming cancer cells in association with the comingled DCs. In this setting, only the *H2kb* wild-type cancer cells express H-2Kb.

The tumor implants were harvested 8 d postinjection (a time window that enabled recovering sufficient numbers of transduced DCs for analysis) and processed for flow cytometry. Briefly, the matrigel implants were excised and made into single-cell suspensions by collagenase IV (0.2 mg/ml, Worthington), dispase (2 mg/ml, Life Technologies), and DNaseI (0.1 mg/ml, New England BioLabs) treatment in IMDM medium. After 30 min at 37 °C in a shaking thermoblock, the cell suspensions were filtered and washed in PBS containing 2 mM EDTA and 2% FBS. Matrigel-derived cell suspensions were incubated with conjugated antibodies against H-2Kb and cell-specific markers (see **Supplementary Table 3** for details) in blocking solution. Before flow cytometry, the cells were resuspended in DAPI to exclude dead cells.

Statistics and reproducibility. Information on the study outline and sample size is presented in the main text, methods, figures, and figure legends. For experiments involving cell cultures aimed to analyze cell behavior, such as T-cell proliferation or cell-binging assays, we used two or three independent cell cultures per condition. In these cases, each cell culture was regarded as a biological replicate, and statistics were derived when at least three independent cell cultures were analyzed per condition. In other cases, we analyzed the variability of defined cellular parameters (e.g., the intracellular localization of internalized EVs) at the single-cell level. In these cases, individual cells were regarded as independent biological replicates, and statistics were derived when at least eight independent cells were analyzed per condition.

Studies involving mice were performed once. Each study was designed to use the minimum number of mice required to obtain informative results (that is, quantitative data amenable to statistical analysis). No specific statistical tests were used to predetermine the sample size; our previous experience with subcutaneous tumor models provided guidance. Tumor-bearing mice were randomized before treatment by allocating mice bearing tumors ranked by volume to alternate treatment groups. We further verified that the mean tumor volume before treatment was comparable in the different experimental groups.

Experiments were not performed blinded; however, data acquisition was blinded in most of the cases. No data were excluded from analysis. Detailed information about the statistical methods is indicated in each figure legend. For comparison between two experimental groups, we applied an unpaired two-sided Student's *t*-test. When multiple groups were compared, we applied a one-way ANOVA analysis with either Dunnett's correction, for comparing multiple groups to a specific control group within a data set, or Tukey's correction, for multiple comparisons within a data set. We applied a two-way ANOVA followed by either Tukey's correction for multiple comparisons or Sidak's correction for two comparisons. Error bars show the s.e.m. The number and type of replicates for each experiment is indicated in the figure legends.

Life Sciences Reporting Summary. Further information on experimental design is available in the **Life Sciences Reporting Summary**.

Data availability. Source data for all the graphical representations reported in the manuscript have been provided in **Supplementary Table 2**. All other data supporting the findings of this study are available from the corresponding authors on request.

20. Zhou, H. *et al. J. Biol. Chem.* **286**, 31676–31683 (2011).
21. Squadrito, M.L. *et al. Cell Rep.* **1**, 141–154 (2012).
22. Horwacik, I. *et al. Mol. Cell. Proteomics* **14**, 2577–2590 (2015).
23. Goedhart, J. *et al. Nat. Commun.* **3**, 751 (2012).
24. Leto, S.M. *et al. Clin. Cancer Res.* **21**, 5519–5531 (2015).
25. Koller, B.H., Marrack, P., Kappler, J.W. & Smithies, O. *Science* **248**, 1227–1230 (1990).
26. De Palma, M. & Naldini, L. *Methods Enzymol.* **346**, 514–529 (2002).
27. Chopra, T. *et al. Mol. Cell. Proteomics* **13**, 3014–3028 (2014).
28. Dunn, K.W., Kamocka, M.M. & McDonald, J.H. *Am. J. Physiol. Cell Physiol.* **300**, C723–C742 (2011).

nature research

Corresponding Author: Michele De Palma

Date: Nov 19, 2017

Life Sciences Reporting Summary

Nature Research wishes to improve the reproducibility of the work we publish. This form is published with all life science papers and is intended to promote consistency and transparency in reporting. All life sciences submissions use this form; while some list items might not apply to an individual manuscript, all fields must be completed for clarity.

For further information on the points included in this form, see Reporting Life Sciences Research. For further information on Nature Research policies, including our data availability policy, see Authors & Referees and the Editorial Policy Checklist.

Experimental design

1. Sample size

   Describe how sample size was determined.

   For experiments involving cell cultures aimed to analyze cell behavior, such as T-cell proliferation or cell-binging assays, we used 2 or 3 independent cell cultures per condition. In these cases, each cell culture was regarded as a biological replicate and statistics were derived when at least 3 independent cell cultures were analyzed per condition. In other cases, we analyzed the variability of defined cellular parameters (for example, the intracellular localization of internalized EVs) at the single cell level. In these cases, individual cells were regarded as independent biological replicates and statistics were derived when at least 8 independent cells were analyzed per condition. Studies involving mice were performed once. Each study was designed to use the minimum number of mice required to obtain informative results (that is, quantitative data amenable to statistical analysis). No specific statistical tests were used to predetermine the sample size; our previous experience with subcutaneous tumor models provided guidance about the adequate number of mice that would provide statistically significant results.

2. Data exclusions

   Describe any data exclusions.

   No data were excluded from the analysis.

3. Replication

   Describe whether the experimental findings were reliably reproduced.

   Most experiments were repeated at least 2 times. Studies involving mice were performed once. Each study was designed to use the minimum number of mice required to obtain informative and statistically significant results.

4. Randomization

   Describe how samples/organisms/participants were allocated into experimental groups.

   Tumor-bearing mice were randomized before treatment by allocating mice bearing tumors ranked by volume to alternate treatment groups. We further verified that the mean tumor volume before treatment was comparable in the different experimental groups.

5. Blinding

   Describe whether the investigators were blinded to group allocation during data collection and/or analysis.

   Experiments were not performed blinded, however, data acquisition was blinded in most of the cases.

Note: all studies involving animals and/or human research participants must disclose whether blinding and randomization were used.

Nature Methods: doi:10.1038/nmeth.4579

6. Statistical parameters

For all figures and tables that use statistical methods, confirm that the following items are present in relevant figure legends (or the Methods section if additional space is needed).

n/a	Confirmed	
☐	☒	The exact sample size (*n*) for each experimental group/condition, given as a discrete number and unit of measurement (animals, litters, cultures, etc.)
☐	☒	A description of how samples were collected, noting whether measurements were taken from distinct samples or whether the same sample was measured repeatedly.
☐	☒	A statement indicating how many times each experiment was replicated
☐	☒	The statistical test(s) used and whether they are one- or two-sided (note: only common tests should be described solely by name; more complex techniques should be described in the Methods section)
☐	☒	A description of any assumptions or corrections, such as an adjustment for multiple comparisons
☐	☒	The test results (e.g. *p* values) given as exact values whenever possible and with confidence intervals noted
☐	☒	A summary of the descriptive statistics, including central tendency (e.g. median, mean) and variation (e.g. standard deviation, interquartile range)
☐	☒	Clearly defined error bars

See the web collection on statistics for biologists for further resources and guidance.

Software

Policy information about availability of computer code

7. Software

Describe the software used to analyze the data in this study.

Data presentation and statistical analysis were performed with GraphPad Prism v6.0h for Mac. For confocal images we employed ImageJ v2.0.0. In flow cytometry experiments, we have employed the Diva BD Bioscience software for data collection and FlowJo, LLC V10.1 for data analysis. Mass Spectrometry data were analysed by Scaffold 4.8.4.

For all studies, we encourage code deposition in a community repository (e.g. GitHub). Authors must make computer code available to editors and reviewers upon request. The *Nature Methods* guidance for providing algorithms and software for publication may be useful for any submission.

Materials and reagents

Policy information about availability of materials

8. Materials availability

Indicate whether there are restrictions on availability of unique materials or if these materials are only available for distribution by a for-profit company.

All the materials employed are available from commercial sources with the exception of immortalized murine bone marrow derived macrophages (iBMM) and lentiviral vectors, which can be made available upon reasonable request.

9. Antibodies

Describe the antibodies used and how they were validated for use in the system under study (i.e. assay and species).

Only commercially available and routinely used antibodies have been used in this study. For each antibody, we provided clone number, provider and working dilution.

Nature Methods: doi:10.1038/nmeth.4579

10. Eukaryotic cell lines

a. State the source of each eukaryotic cell line used.

Murine monocytic cells (P388D1), human embryonic kidney cells (293T), MC38 colon carcinoma cells, and iBMM cells, have been previously used in our laboratory.
MC38-OVA cells were provided by Nicole Haynes (Peter MacCallum Cancer Center, Melbourne, AU).
SM1-OVA cells were provided by Antony Ribas (University of California, Los Angeles, CA).

b. Describe the method of cell line authentication used.

The original stocks of tumor cell lines were authenticated, but we did not perform further authentication analysis in the past few years. However, we are confident that the cell lines used are authentic, as their growth behavior and immune infiltrates are consistent with those we observed historically as well as with data reported by others in the literature.

c. Report whether the cell lines were tested for mycoplasma contamination.

All cell lines have resulted negative for Mycoplasma in routine tests.

d. If any of the cell lines used in the paper are listed in the database of commonly misidentified cell lines maintained by ICLAC, provide a scientific rationale for their use.

No commonly misidentified cell lines have been used.

Animals and human research participants

Policy information about studies involving animals; when reporting animal research, follow the ARRIVE guidelines

11. Description of research animals

Provide details on animals and/or animal-derived materials used in the study.

All mice used in this study were maintained in a pathogen-free barrier animal facility according to the Swiss regulations for animal care and experimental research.
OT-I TCR transgenic mice were available at EPFL.
C57Bl6/J, FVB/n and Nod SCID gamma (NSG) mice were purchased from Charles River Laboratory (L'Arbresle, France).
Tibias and femurs from B2m-deficient mice were a gift of Greta Guarda (University of Lausanne, UNIL).

Cancer cells (with or without dendritic cells) were injected subcutaneously into the right flank of 6-week old C57Bl6/J mice of both sexes.

Policy information about studies involving human research participants

12. Description of human research participants

Describe the covariate-relevant population characteristics of the human research participants.

This study did not involve any human-related materials.

Nature Methods: doi:10.1038/nmeth.4579

nature research

Corresponding Author: Michele De Palma

Date: Jun 5, 2017

Flow Cytometry Reporting Summary

Form fields will expand as needed. Please do not leave fields blank.

Data presentation

For all flow cytometry data, confirm that:

☒ 1. The axis labels state the marker and fluorochrome used (e.g. CD4-FITC).

☒ 2. The axis scales are clearly visible. Include numbers along axes only for bottom left plot of group (a 'group' is an analysis of identical markers).

☒ 3. All plots are contour plots with outliers or pseudocolor plots.

☒ 4. A numerical value for number of cells or percentage (with statistics) is provided.

Methodological details

5. Describe the sample preparation.

Flow cytometry of iBMM and DC cultures
After cell culture, iBMMs were detached with trypsin/EDTA, whereas DCs were detached by pipetting. For dLNGFR and B2M analysis, the cells were stained with directly conjugated primary antibodies (see Supplementary Table 3 for details) in the presence of blocking solution. For F(ab)2 analysis, the cells were stained with a directly conjugated anti-F(ab)2 antibody (see Supplementary Table 3 for details),, without other antibodies. The cells were finally resuspended in 7AAD-containing wash solution to exclude dead cells.
For EV treatment studies, iBMMs were seeded in 24-well plates (10^5/well) and DCs in 96-well plates (2 x 10^4/well). Cells were incubated with 2 x 10^8 EVs/well (according to NTA analysis), except where indicated otherwise. iBMMs were detached with trypsin/EDTA, whereas DCs were detached by pipetting; the cells were then washed with a mild acid solution (50 mM acetic acid) to remove EVs attached to the cell membrane. Before flow cytometry analysis of direct PKH67, mCh or mTq fluorescence, the cells were stained with an APC-conjugated anti-dLNGFR antibody in the presence of Fc block. For H-2Kb analysis the cells were stained with APC-conjugated anti-dLNGFR and PE-conjugated anti-H-2Kb antibodies in the presence of Fc block (see Supplementary Table 3 for details). The cells were finally resuspended in 7AAD-containing wash solution to exclude dead cells.

Flow cytometry of cancer cell lines
After cell culture, cancer cells were detached with trypsin/EDTA. For B2M, H-2Kb, HER2 and GD2 analysis, the cells were stained with directly-conjugated primary antibodies (see Supplementary Table 3 for details) in the presence of Fc block. Before analysis, the cells were resuspended in 7AAD-containing wash solution.

Flow cytometry of EVs
To analyze HER2 on EVs, we stained 10^9-10^10 EVs in 100 µl of PBS containing an AlexaFluor-647–conjugated anti-HER2 antibody in the presence of Fc block. After 15 min at 4˚C, the preparations

Nature Methods: doi:10.1038/nmeth.4579

were washed and the EVs isolated by ultracentrifugation, as described above. EVs were resuspended in PBS and analyzed using an LSR2 device (BD Bioscience).

6. Identify the instrument used for data collection.

Flow cytometry used a LSR2 device (BD Bioscience); in all experiments, the fluorescence of GFP, mTq and mCh was directly detected using the 488-525/50, 450-450/50 and 561-610/20 channels, respectively.

7. Describe the software used to collect and analyze the flow cytometry data.

We employed the BD FACSDiva Software V8.0.1 (build2014 07 03 11 47) for data collection, and FlowJo LLC V10.1 for data analysis.

8. Describe the abundance of the relevant cell populations within post-sort fractions.

Isolation of CD8+ OT-I cells
CD8+ OT-I cells were isolated from OT-I TCR transgenic mice, which produce MHC class I-restricted, ovalbumin (OVA)-specific CD8+ T cells. The spleens were collected under sterile conditions, smashed and filtered by using gravity-driven 70 µm cell strainers to obtain single cell suspensions. We depleted CD11c+ cells with anti-CD11c microbeads (Miltenyi Biotech) and an autoMACS Pro separator apparatus. Subsequently, we positively selected CD8+ T cells using anti-CD8 microbeads (Miltenyi Biotech). CD8+ T cells were maintained in RPMI medium complemented with FBS, L-glutamine and penicillin-streptomycin, non-essential amino acid solution (Sigma), sodium pyruvate (1 mM, Gibco) and 2-mercaptoethanol (25 µM, Gibco).
CD8+ T cell purity was above 90% in all experiments.

9. Describe the gating strategy used.

dLNGFR+ DCs and dextramer+CD8+ T cells were first gated based on physical parameters to identify single cells (i.e. FSA-A and FSA-H, FSA-A and SSC-H).
dLNGFR+ DCs from matrigel implants were identified as (1) CD45+ DAPI+ and (2) dLNGFR+GFP– cells.
Splenic CD8+ T cells were identified as (1) 7AAD–, to exclude death cells; and (2) CD8+CD45+CD11b–.
Gates involving fluorochromes were designed based on protein levels on KO cells, as shown in Supplementary Figures 6b, 7b, 7c and 8d, or based on fluorescence minus one (FMO) controls, as shown in Supplementary Figure 13.

Tick this box to confirm that a figure exemplifying the gating strategy is provided in the Supplementary Information. ☒

Nature Methods: doi:10.1038/nmeth.4579

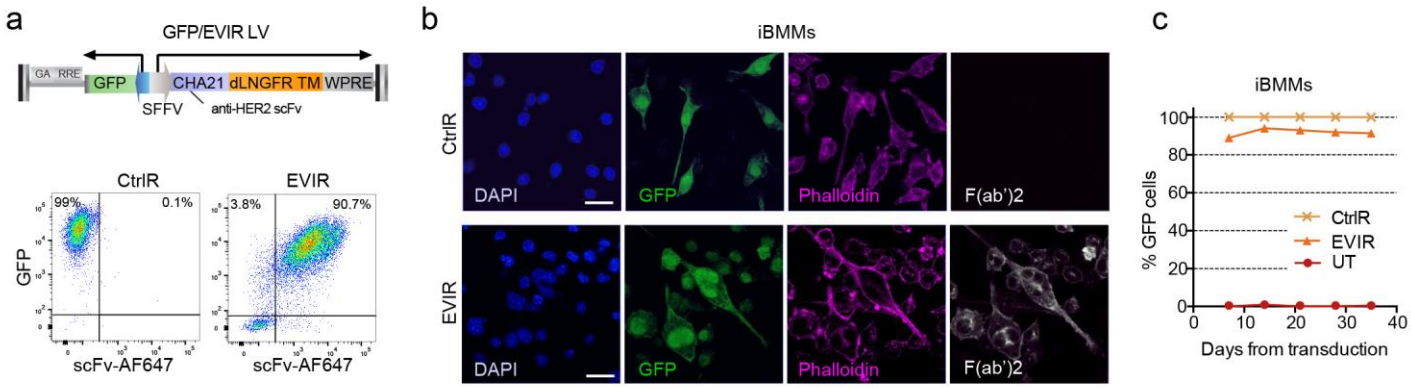

Supplementary Figure 1

Transduced monocytic cells stably express an anti-HER2 EVIR

a) The top panel shows a schematic of the bidirectional lentiviral vector (LV) used to coordinately express the CtrlR or anti-HER2 EVIR, and GFP. The bottom panels illustrate representative flow cytometry dot plots showing expression of the EVIR, stained with an anti-F(ab')$_2$ antibody, and GFP, in iBMM-CtrlR and iBMM-EVIR cells. The cells were analyzed 7 days post-transduction. One cell culture *per* LV type is shown; data are representative of 3 independent transduction experiments.

(**b**) Individual confocal images showing anti-scFv immunostaining (white), direct GFP fluorescence (green), actin fibers stained with phalloidin (magenta), and nuclear staining with DAPI (blue), in iBMM-CtrlR and anti-HER2 iBMM-EVIR cells. See Figure 1b for experimental details. Scale bar, 50 μm.

(**c**) Flow cytometry analysis of GFP expression in untransduced (UT) iBMMs, anti-HER2 iBMM-EVIR and iBMM-CtrlR cells. The iBMMs were passaged for 11 times during the 36 days that followed cell transduction. Data show percentage values. One cell culture *per* LV type is shown. The experiment was performed one time.

Numerical values for the experiments with quantitative data are presented in **Supplementary Table 2**.

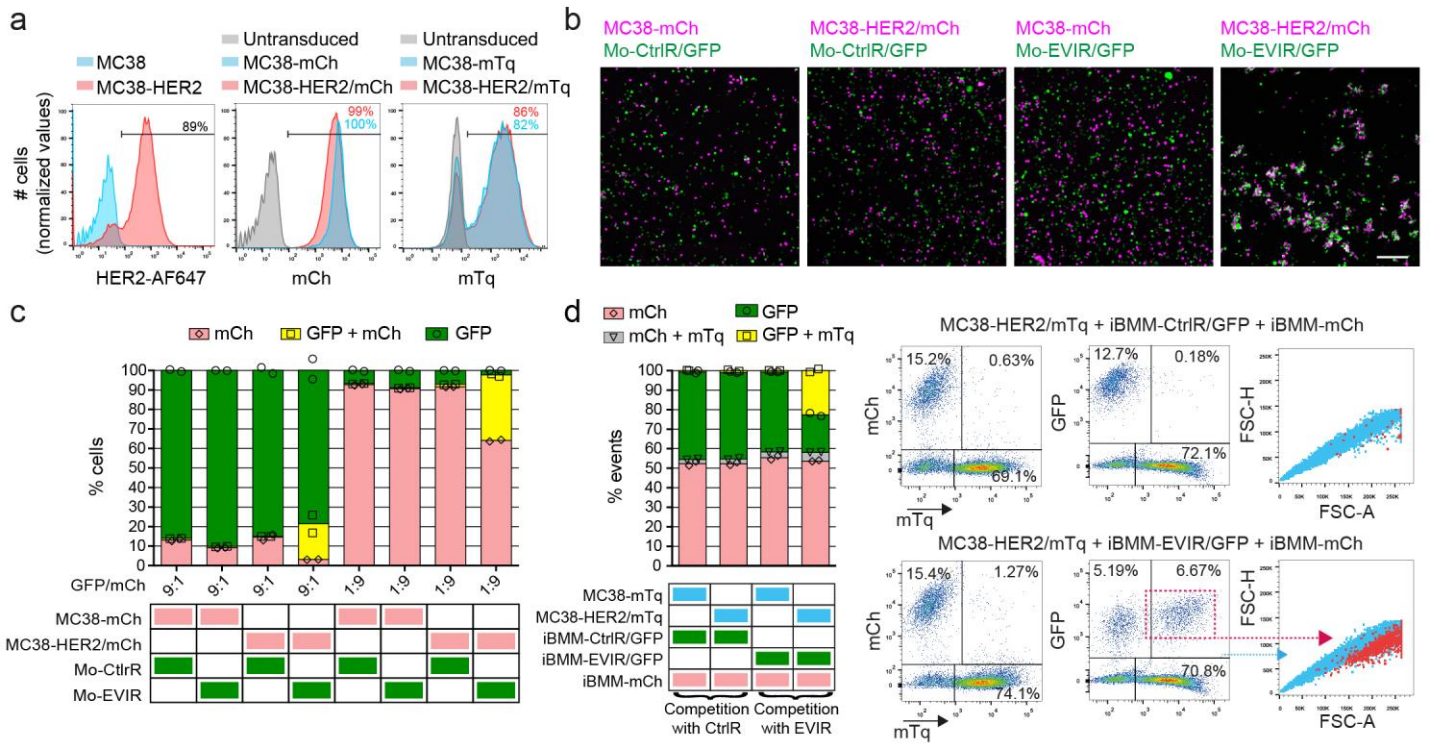

Supplementary Figure 2

Anti-HER2 EVIR-expressing monocytic cells avidly adhere to HER2$^+$ cancer cells

(**a**) Flow cytometry histograms of HER2, mCh and mTq in MC38 cells transduced as indicated. One cell culture *per* LV type is shown; data are representative of at least 2 independent transduction experiments.

(**b**) Cell binding assay using Mo-EVIR/GFP (or control Mo-CtrlR/GFP) and MC38-HER2/mCh (or control MC38-mCh) cells incubated in suspension for 20 min at 1:1 ratio. The figure shows representative images of MC38 cells (mCh$^+$, magenta) and monocytes (GFP$^+$, green) transduced as indicated and imaged before flow cytometry; see Figure 1c for experimental details. Scale bar, 200 µm.

(**c**) Cell binding assay using Mo-EVIR/GFP (or control Mo-CtrlR/GFP) and MC38-HER2/mCh (or control MC38-mCh) cells incubated in suspension for 20 min at either 9:1 or 1:9 ratio. Data show the proportion of cells that appear either as single cells (green or pink, representing monocytes and MC38 cells, respectively) or in clusters (yellow, representing monocytes bound to MC38 cells), according to flow cytometry analysis. Data indicate mean values of two independent cell cultures *per* condition.

(**d**) Co-culture of iBMM-EVIR/GFP (or control iBMM-CtrlR/GFP), MC38-HER2/mTq (or control MC38-mTq), and iBMM-mCh cells under adherent conditions for 24 h before analysis. The left panel shows flow cytometry analysis of the percentage of events representing iBMMs either as single cells (green or pink) or in clusters with MC38 cells (yellow or grey); mean values of two independent cell cultures *per* condition are shown. The right panel shows representative flow cytometry dot plots. mTq/GFP double-positive events (clusters of iBMM-EVIR/GFP and MC38-HER2/mTq cells) fall in the doublet/aggregate area (red) based on FSC-A and FSC-H physical parameters.

Numerical values for the experiments with quantitative data are presented in **Supplementary Table 2**.

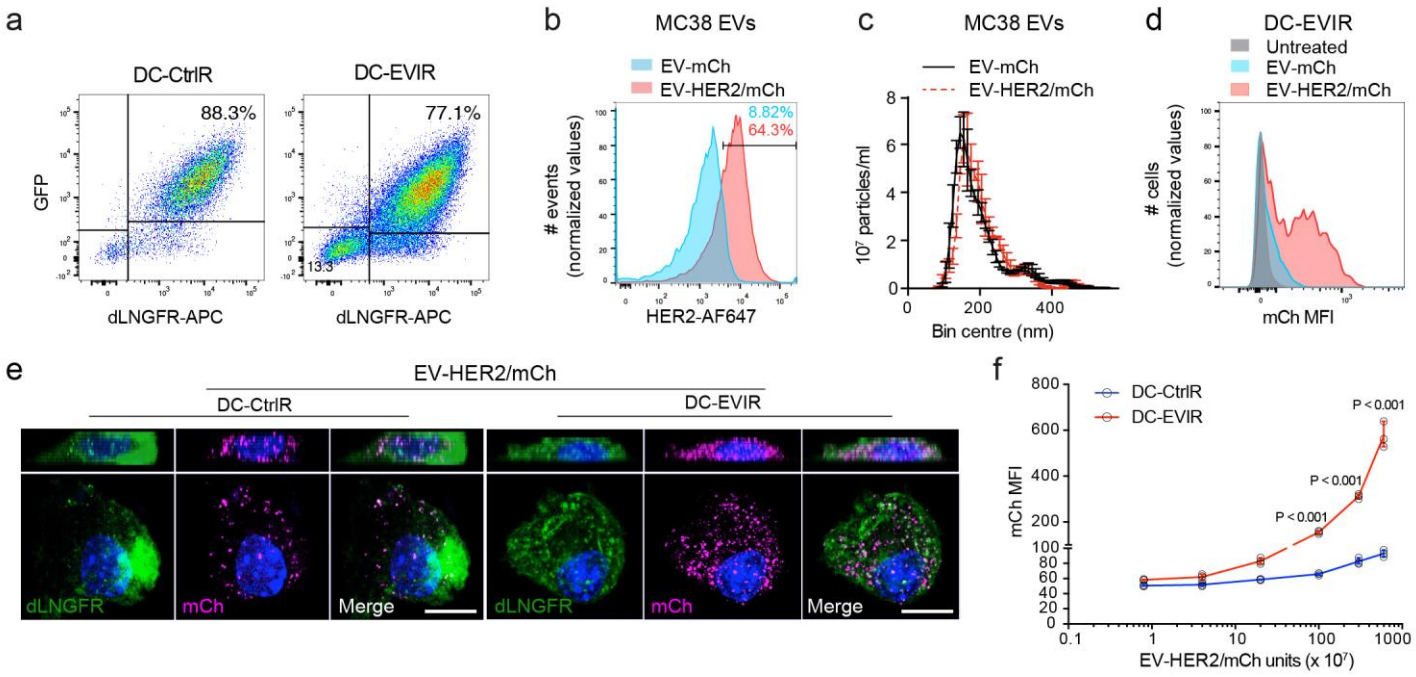

Supplementary Figure 3

DCs transduced with an anti-HER2 EVIR capture and internalize HER2$^+$ EVs

(**a**) Representative flow cytometry dot plots of GFP and EVIR (stained with an anti-dLNGFR antibody) expression in DC-CtrlR and DC-EVIR cells. One cell culture *per* LV type is shown; data are representative of 3 independent cell cultures.

(**b**) Representative flow cytometry histograms of HER2 expression in EV-mCh and EV-HER2/mCh. One EV preparation *per* type is shown; data are representative of 2 independent EV preparations.

(**c**) Size distribution of EV-mCh and EV-HER2/mCh, determined by nanoparticle tracking analysis (NTA). Data show mean values ± SEM (n=3 technical measurements of one EV preparation *per* type). Data are representative of 3 independent EV preparations.

(**d**) Flow cytometry analysis of mCh in DC-EVIR either untreated or treated with EV-mCh or EV-HER2/mCh. Data are representative of 3 independent cell cultures *per* condition.

(**e**) Representative three-dimensional projections of confocal z-stack images showing nuclear DAPI (blue), anti-dLNGFR (green) and anti-mCh (magenta) immunostaining in DC-CtrlR and anti-HER2 DC-EVIR incubated for 2 h with MC38-HER2/mCh EVs. Scale bar, 10 µm. Images are representative of at least 30 cells per condition, analyzed from 3 independent experiments.

(**f**) Dose-response analysis of the median fluorescence intensity (MFI) of mCh in DC-CtrlR and DC-EVIR, either untreated or treated with EV-mCh or EV-HER2/mCh, and analyzed by flow cytometry. Data show mean values ± SEM (n=3 independent cell cultures *per* condition). Statistical analysis by two-way ANOVA with Sidak's multiple comparison test. The experiment was performed one time.

Numerical values for the experiments with quantitative data are presented in **Supplementary Table 2**.

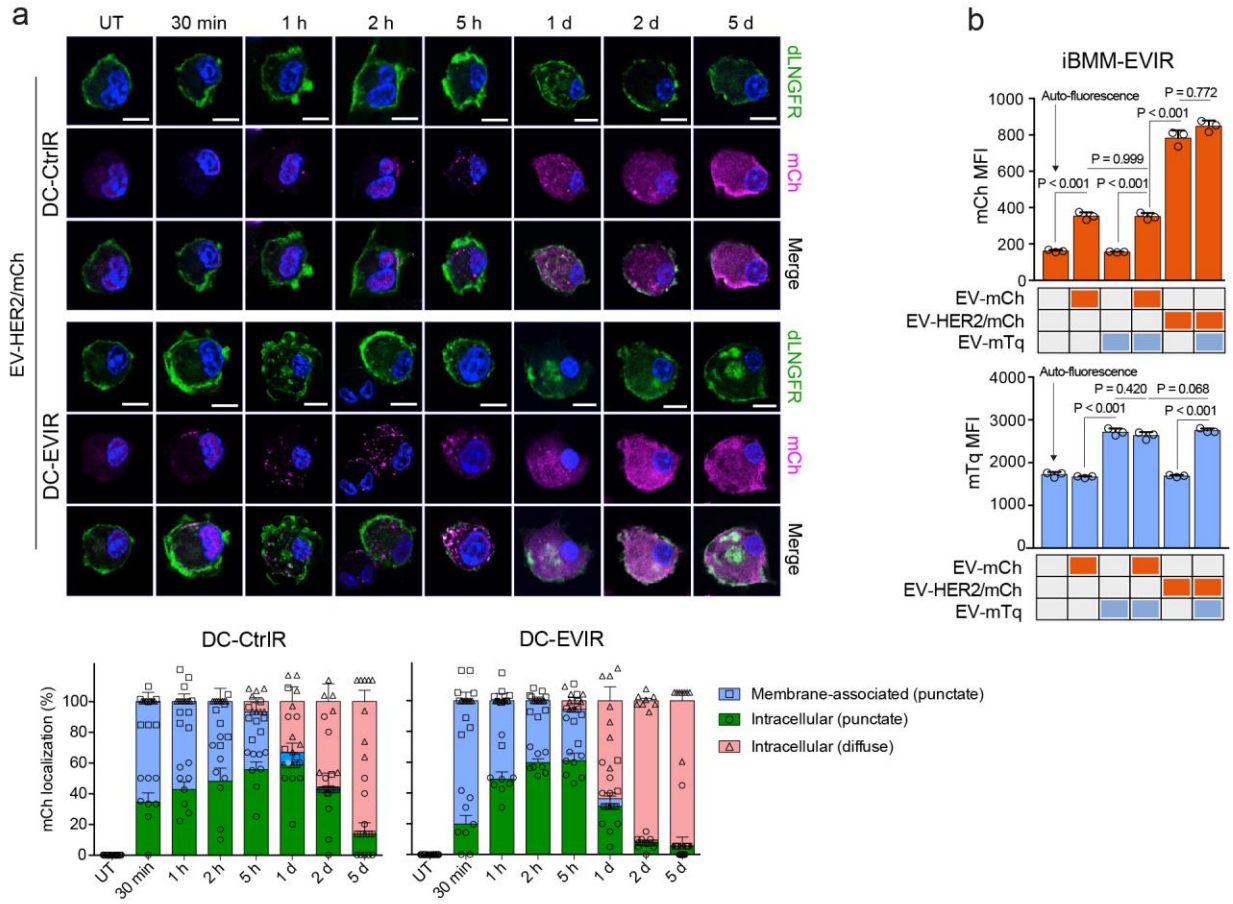

Supplementary Figure 4

DCs transduced with an anti-HER2 EVIR show accelerated kinetics of EV and mCh internalization

(**a**) Time course analysis of mCh localization in DC-EVIR or DC-CtrlR cells incubated with EV-HER2/mCh. The top panel shows representative confocal images of randomly selected dLNGFR$^+$ cells, analyzed at the indicated time points after exposure to EVs. Data show anti-dLNGFR (green) and anti-mCh (magenta) immunostaining, and nuclear staining with DAPI (blue). Scale bar, 10 µm. The bottom panel shows analysis and quantification of the subcellular localization of the mCh signal in DC-CtrlR and DC-EVIR cells. Data show percentage values ± SEM (n=8 dLNGFR$^+$ cells randomly selected *per* time point and condition). Results derived from individual cells, rather than by averaging different cell culture replicates, are reported in order to illustrate the variability of the parameter of interest (mCh localization in 128 independent cells from one experiment). Results are representative of 2 independent experiments. UT, untreated cells (not incubated with EVs).

(**b**) Flow cytometry analysis of mCh or mTq fluorescence in iBMM-EVIR cells, either untreated or treated with the indicated EV preparations. Data illustrate the MFI of mCh (top) and mTq (bottom), shown as mean values ± SEM (n=3 independent cell cultures *per* condition). Statistical analysis by one-way ANOVA with Tukey's multiple comparison test. Numerical values for the experiments with quantitative data are presented in **Supplementary Table 2**.

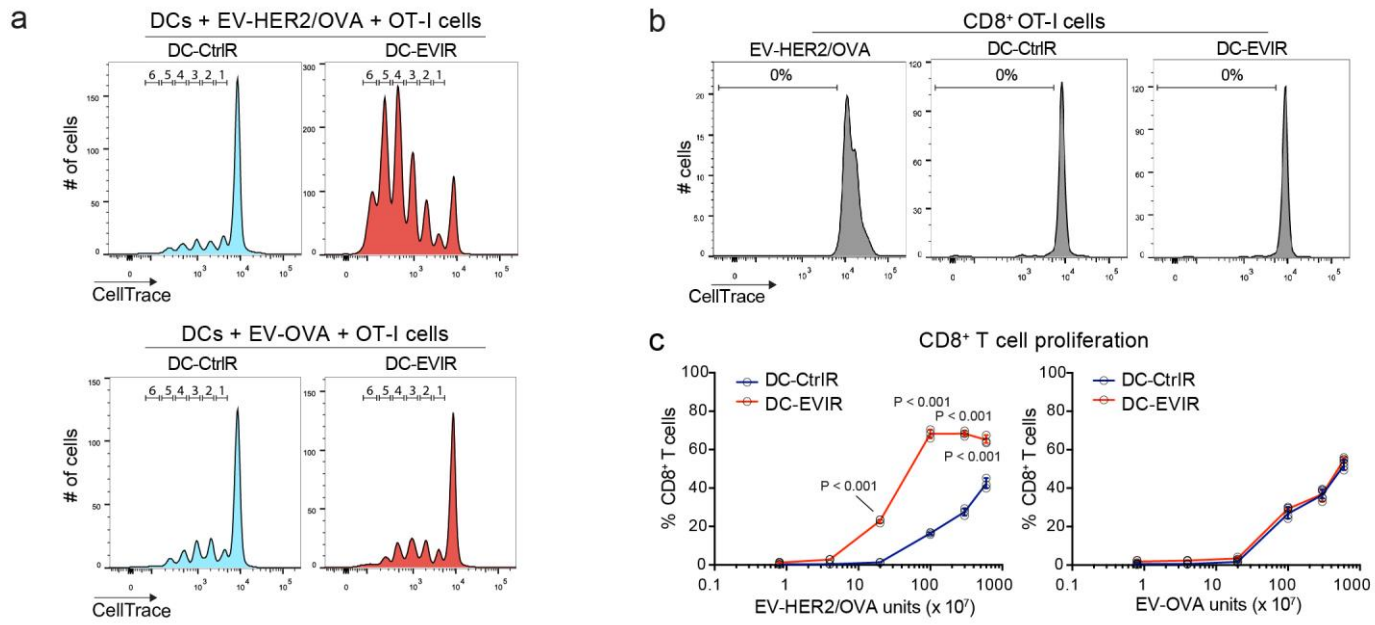

Supplementary Figure 5

DC-EVIR cells promote T cell proliferation

(**a**) Flow cytometry analysis of CD8$^+$ OT-I proliferation, assessed by CellTrace dilution, analyzed after their co-culture with DC-CtrlR or DC-EVIR cells exposed to EV-HER2/OVA (top panels) or EV-OVA (bottom panels). Data show representative flow cytometry histograms of 3 independent cell cultures *per* condition (see Figure 1e for quantitative data).

(**b**) Flow cytometry analysis of CD8$^+$ OT-I proliferation, assessed by CellTrace dilution, analyzed after treatment with EV-HER2/OVA in the absence of DCs, or after co-culture with DC-EVIR or DC-CtrlR cells and without EVs. Data show representative flow cytometry histograms of 3 independent cell cultures *per* condition.

(**c**) Dose-response of CD8$^+$ OT-I cell proliferation, assessed by CellTrace dilution, after co-culture with DC-EVIR or DC-CtrlR in the presence of EV-HER2/OVA (left) or EV-OVA (right). Data show mean values ± SEM (n=3 independent cell cultures *per* condition). Statistical analysis by two-way ANOVA with Sidaks's multiple comparison test.

Numerical values for the experiments with quantitative data are presented in **Supplementary Table 2**.

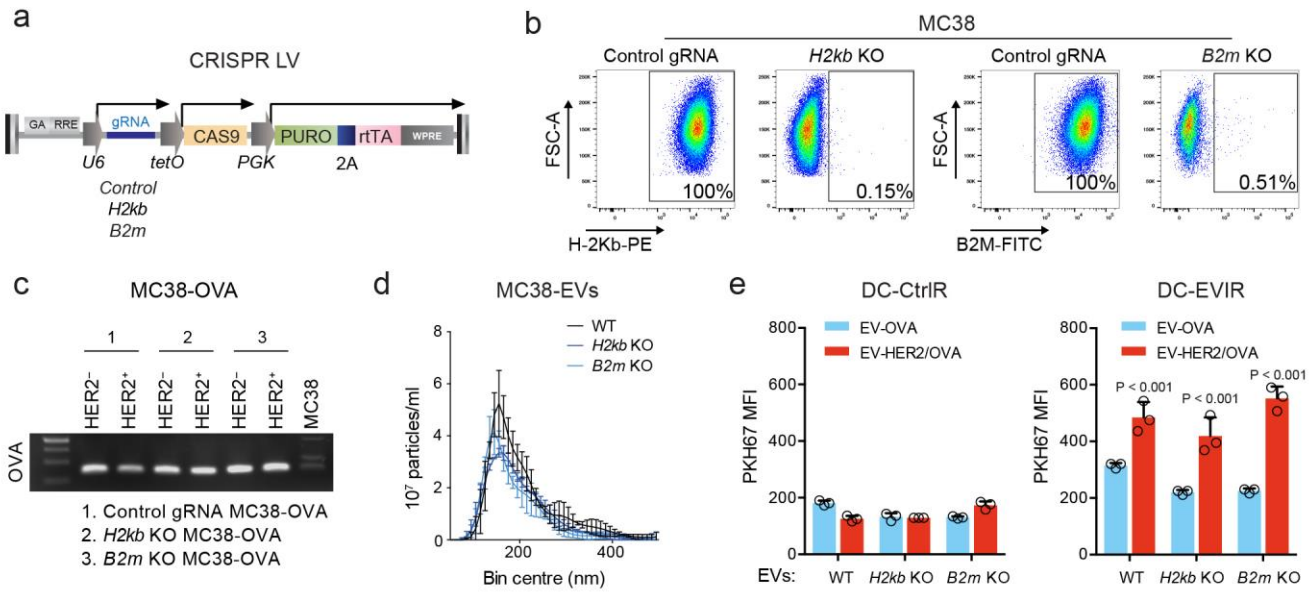

Supplementary Figure 6

An anti-HER2 EVIR enhances EV-uptake by MHCI-deficient DCs

(**a**) Schematic representation of the proviral CRISPR LV, which contains a control gRNA or a gRNA targeting *H2kb* or *B2m*, along with puromycin (PURO) resistance and inducible CAS9 transgenes.

(**b**) Flow cytometry dot plots showing H-2Kb or B2M expression in MC38 cells transduced with a LV without gRNA (control) or containing a gRNA either targeting *H2kb* or *B2m*. The analysis shows cell clones that have been selected for subsequent studies.

(**c**) PCR analysis of genomic OVA in the indicated MC38 cell lines. The analysis shows cell clones that have been selected for subsequent studies.

(**d**) Size distribution of *H2kb*- and *B2m*-deficient MC38-EVs, as determined by NTA. Data show mean values ± SEM (n=3 technical measurements of one EV preparation *per* type). Data are representative of 2 independent EV preparations.

(**e**) Flow cytometry showing the MFI of PKH67 in DC-CtrlR and DC-EVIR treated with PKH67-labeled, wild-type (WT, *H2kb*-proficient), *H2kb*- or *B2m*-deficient EVs that had been isolated from either MC38 or MC38-HER2 cells, as indicated. DCs were analyzed 24 h after exposure to EVs. Data show mean values ± SEM (n=3 independent cell cultures *per* condition); statistical analysis by two-way ANOVA with Sidak's multiple comparison test.

Numerical values for the experiments with quantitative data are presented in **Supplementary Table 2**.

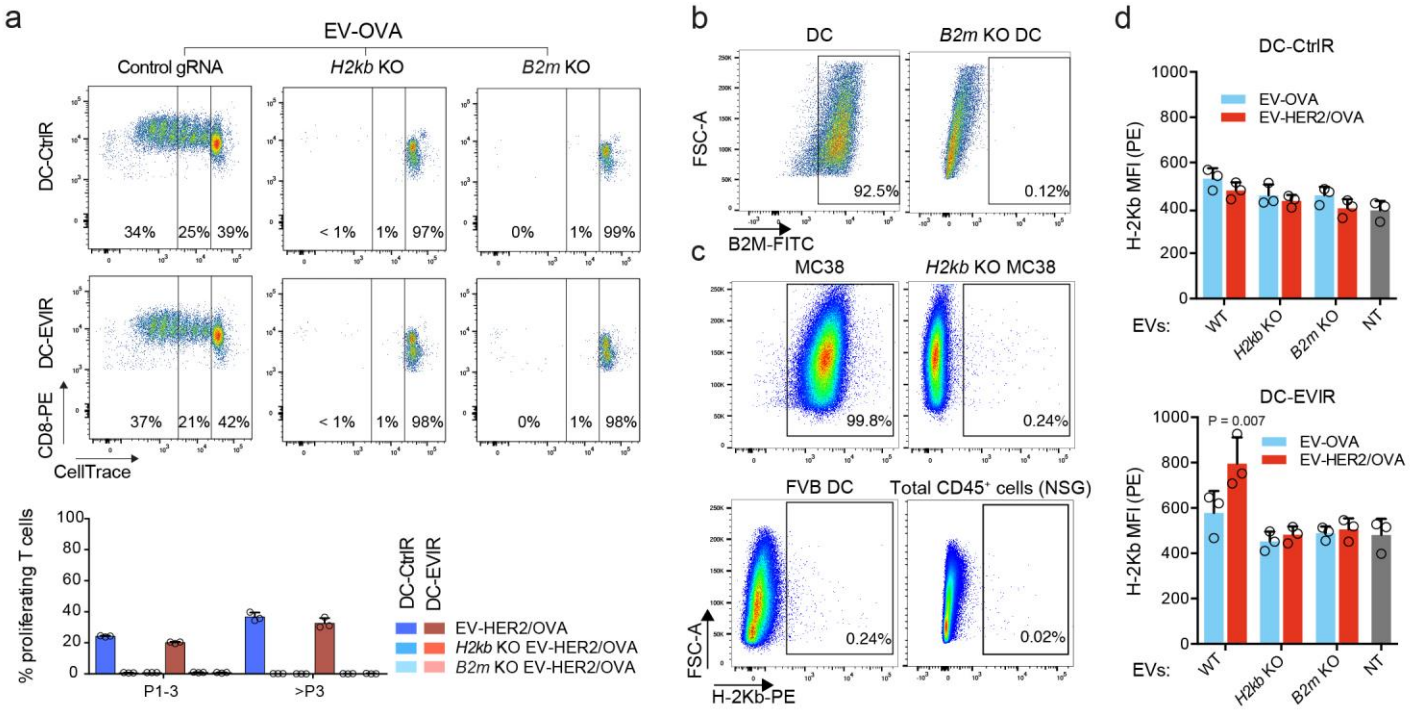

Supplementary Figure 7

An anti-HER2 EVIR enhances EV uptake by DCs and cross-dressing with MHCI/antigen complexes

(**a**) Flow cytometry analysis of $CD8^+$ OT-I proliferation, assessed by CellTrace dilution, after co-culture with DC-CtrlR or anti-HER2 DC-EVIR cells, and EV-OVA (not containing HER2). The top panels show representative flow cytometry dot plots. The bottom panel shows the percentage of $CD8^+$ OT-I cells that completed 1 to 3 (P1-3) or more than 3 (P>3) cell cycles. Data show mean percentage values ± SEM (n=3 independent cell cultures *per* condition).

(**b, c**) Flow cytometry dot plots showing B2M (b) and H-2Kb (c) expression in the indicated cell types. In (b), "*B2m* KO DC" refers to DCs isolated from the bone marrow of *B2m* KO mice (analysis performed once to verify a genetically-determined phenotype). In (c), "FVB DC" indicates DCs that were differentiated from the bone marrow of FVB/n mice (analysis performed once to verify a genetically-determined phenotype), whereas "Total $CD45^+$ cells (NSG)" indicates all hematopoietic ($CD45^+$) cells retrieved from a matrigel-embedded tumor containing *H2kb* KO MC38 cells and FVB/n DCs (analysis performed on 4 independent cell suspensions, of which one is shown). MHCI-competent bone marrow-derived DCs of C57Bl/6 mice ("DC") and MC38 cancer cells ("MC38") are shown for comparison (analysis performed once to verify a genetically-determined phenotype).

(**d**) Expression of H-2Kb in DCs transduced as indicated and exposed to the indicated EV preparations. Cells were analyzed 24 h after exposure to EVs. Data show mean values ± SEM (n=3 independent cell cultures *per* condition); statistical analysis by two-way ANOVA with Sidak's multiple comparison test.

Numerical values for the experiments with quantitative data are presented in **Supplementary Table 2**.

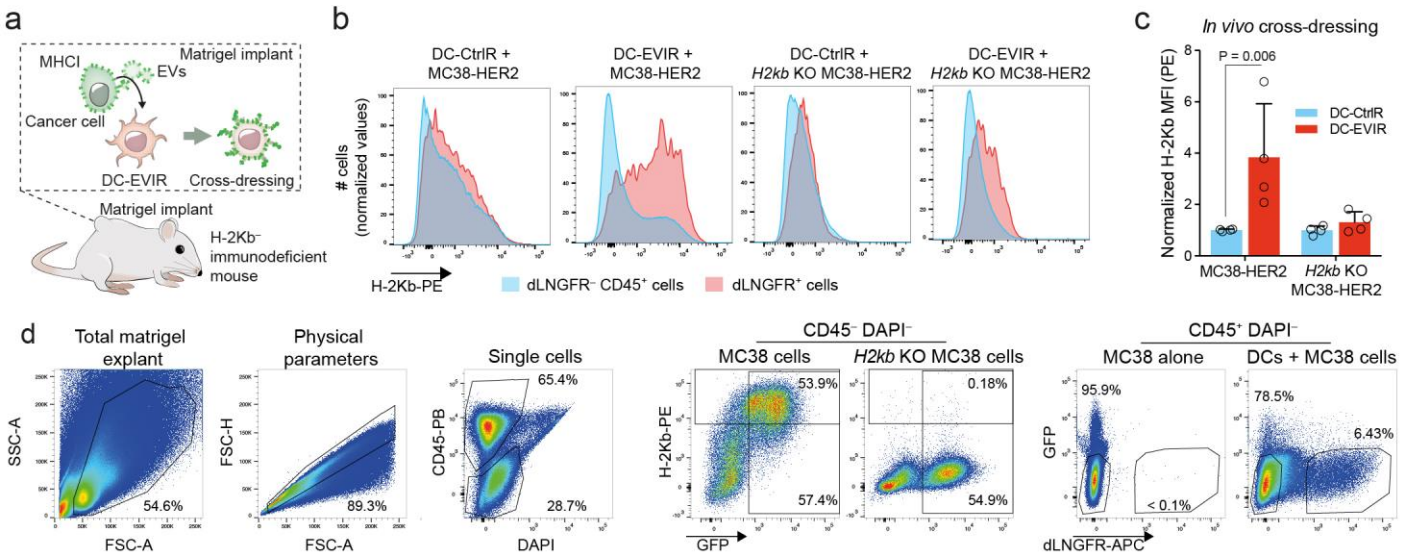

Supplementary Figure 8

An anti-HER2 EVIR promotes DC cross-dressing with MHCI/antigen complexes in a mouse tumor model

(**a-c**) MC38 cancer cells (either *H2kb* wild-type or KO) and *H2kb*-deficient DCs (FVB/n origin) were co-mingled in matrigel plugs implanted in *H2kb*-deficient NSG mice (see Supplementary Figure 7c) and the tumors allowed to grow for 8 days. A schematic representation of the experiment is shown in (a). Panel (b) shows representative flow cytometry analyses of H-2Kb expression in the relevant cell types: dLNGFR$^+$ cells, which represent transduced DC-EVIR or DC-CtrlR cells, and dLNGFR-negative CD45$^+$ cells, which represent non-transduced hematopoietic cells recruited to the matrigel plug from the NSG host. Panel (c) shows analysis of the flow cytometry data. Data show mean values ± SEM (n=4 mice/condition) after normalizing the data to H-2Kb expression in the dLNGFR-negative cells (set to 1); statistical analysis by two-way ANOVA with Sidak's multiple comparison test.

(**d**) Representative flow cytometry dot plots showing the gating strategy employed in (a-c).

Numerical values for the experiments with quantitative data are presented in **Supplementary Table 2**.

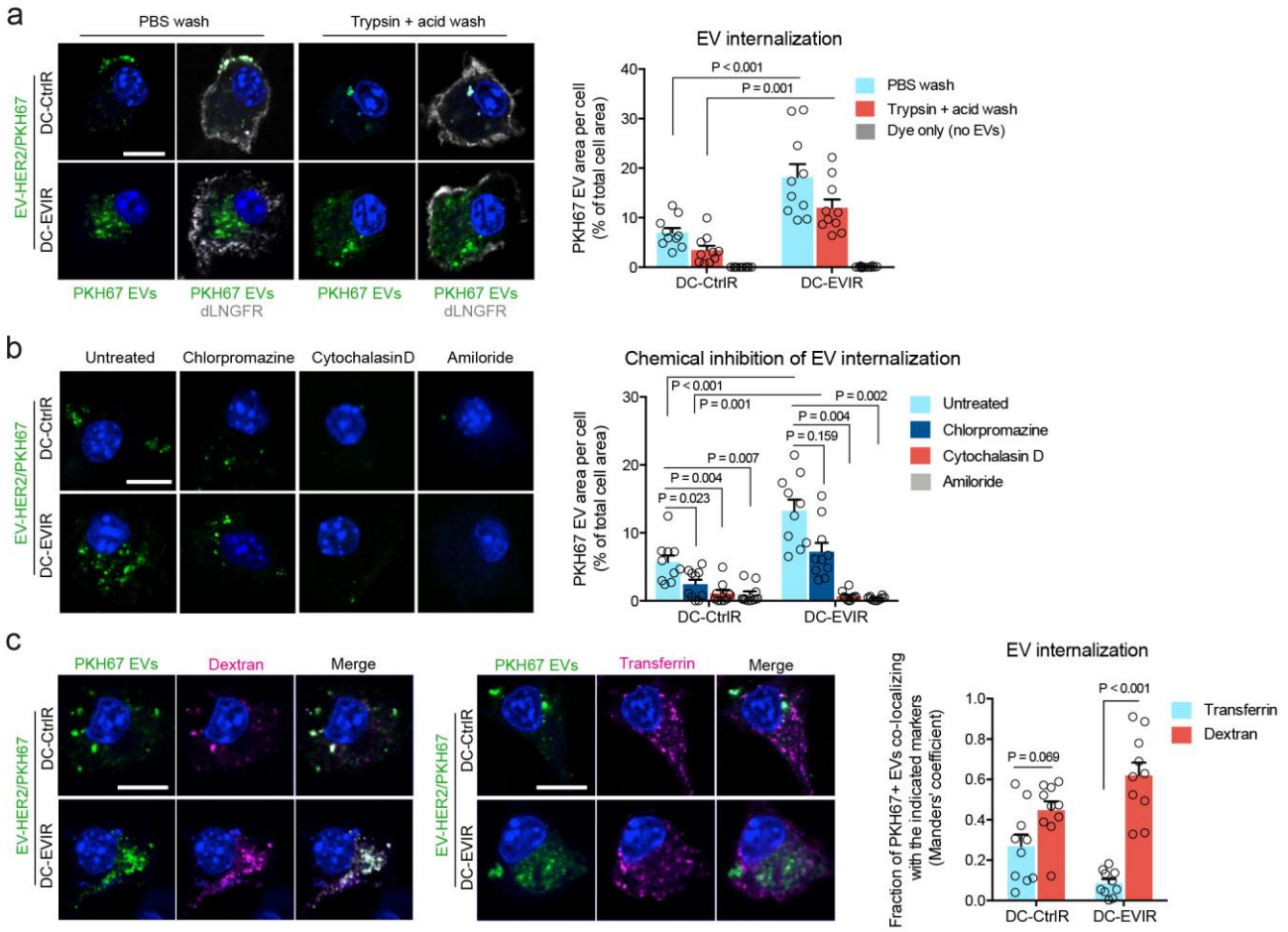

Supplementary Figure 9

An anti-HER2 EVIR promotes EV internalization preferentially through macropinocytosis

(**a**) The left panels show representative confocal images of DC-CtrlR and DC-EVIR after incubation with PKH67-labeled EV-HER2 (green) for 2 h, followed by washing with trypsin and acetate (or PBS), prior to fixation. The cells were stained with anti-dLNGFR antibodies (white) and their nuclei labeled with DAPI (blue). Scale bar, 10 μm. The right panel shows the quantification of the PKH67$^+$ area; the total cell area was determined by dLNGFR$^+$ membrane staining. Data show mean percentage values ± SEM (n=10 dLNGFR$^+$ cells randomly selected *per* condition). Results derived from individual cells, rather than by averaging different cell culture replicates, are reported in order to illustrate the variability of the parameter of interest (PKH67$^+$ area). Statistical analysis by two-way ANOVA with Sidak's multiple comparison test. Results are representative of 2 independent experiments.

(**b**) The left panels show representative confocal images of DC-CtrlR and DC-EVIR treated with the indicated endocytosis inhibitors, followed by incubation with PKH67-labeled EV-HER2 (green) for 2 h, prior to fixation. The cells were stained with anti-dLNGFR antibodies (not shown) and their nuclei labeled with DAPI (blue). Scale bar, 10 μm. The right panel shows the analysis of the PKH67$^+$ area, calculated as in (a). Data show mean percentage values ± SEM (n=10 dLNGFR$^+$ cells randomly selected *per* condition). For statistical analysis, see (a). In addition, one-way ANOVA analysis with Dunnett's multiple comparison test was performed, within either DC-CtrlR or DC-EVIR group, to compare each treatment

condition with the corresponding untreated group. Results are representative of 2 independent experiments.

(**c**) The left panels show representative confocal images of DC-CtrlR and DC-EVIR exposed to PKH67-labelled EVs (green) along with dextran-TRITC (magenta) or transferrin-AF555 (magenta) for 2h, prior to fixation. The cells were stained with anti-dLNGFR antibodies (not shown) and their nuclei labeled with DAPI (blue). Scale bar, 10 μm. The right panel shows co-localization analysis of mCh with the indicated endocytosis marker, measured using the Manders' coefficient. Data show mean values ± SEM (n=10 $dLNGFR^+$ cells randomly selected *per* condition). For statistical analysis, see (a). Results are representative of 2 independent experiments.

Numerical values for the experiments with quantitative data are presented in **Supplementary Table 2**.

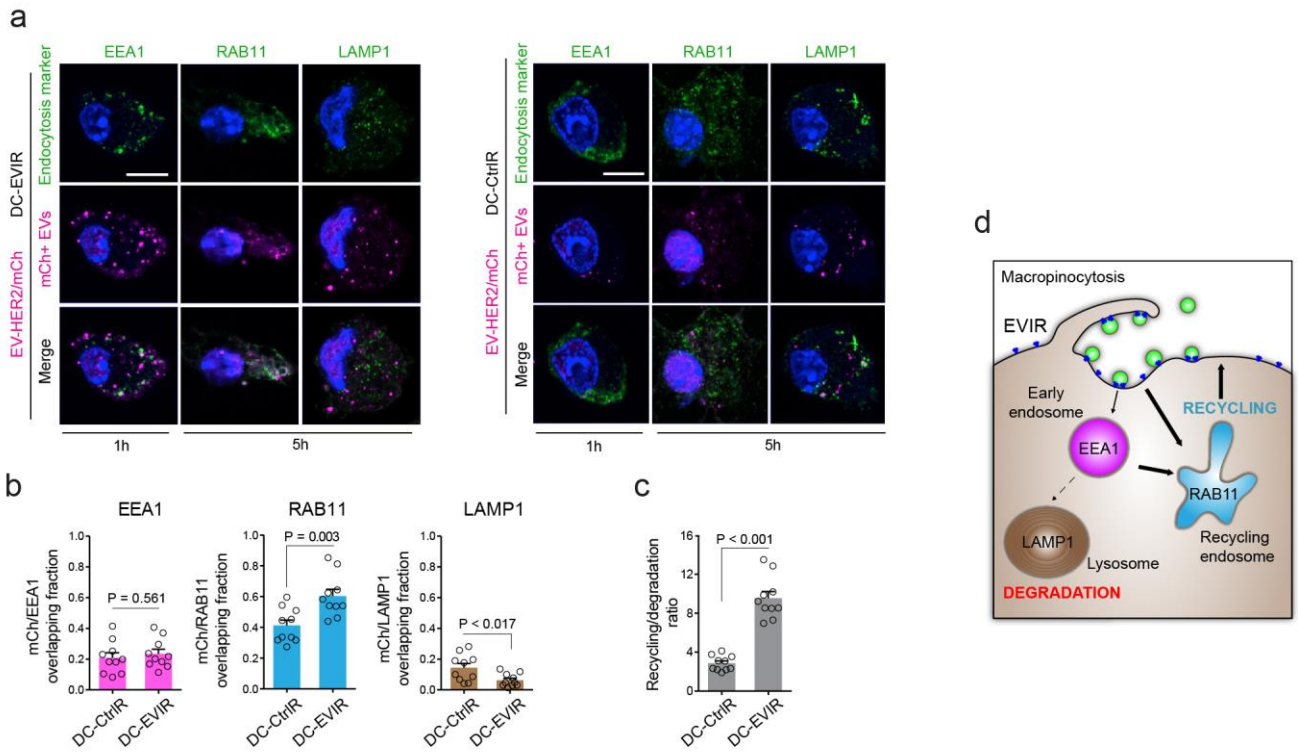

Supplementary Figure 10

An anti-HER2 EVIR encourages EV sorting to recycling endosomes

(**a**) Representative confocal images of DC-EVIR (left) and DC-CtrlR (right) incubated with EV-HER2/mCh (magenta) for 1 or 5 h and immunostained for the indicated endocytic markers (green). The cells were stained with anti-dLNGFR antibodies (not shown) and their nuclei labeled with DAPI (blue). Scale bar, 10 μm. Images are representative of 10 cells randomly selected per condition.

(**b**) Co-localization analysis of mCh and the indicated endocytosis marker, measured using the Manders' coefficient. Data show mean values ± SEM (n=10 cells randomly selected *per* condition). Results derived from individual cells, rather than by averaging different cell culture replicates, are reported in order to illustrate the variability of the parameter of interest (degree of co-localization). Statistical analysis by unpaired two-sided Student's t test. Results are representative of 2 independent experiments.

(**c**) Ratio of EV recycling (in RAB11$^+$ endosomes) over degradation (in LAMP1$^+$ lysosomes), calculated from the data in (b). Statistical analysis as in (b). Results are representative of 2 independent experiments.(**d**) Schematic representation of endocytic pathways relevant to the data shown in panels (a-c).

Numerical values for the experiments with quantitative data are presented in **Supplementary Table 2**.

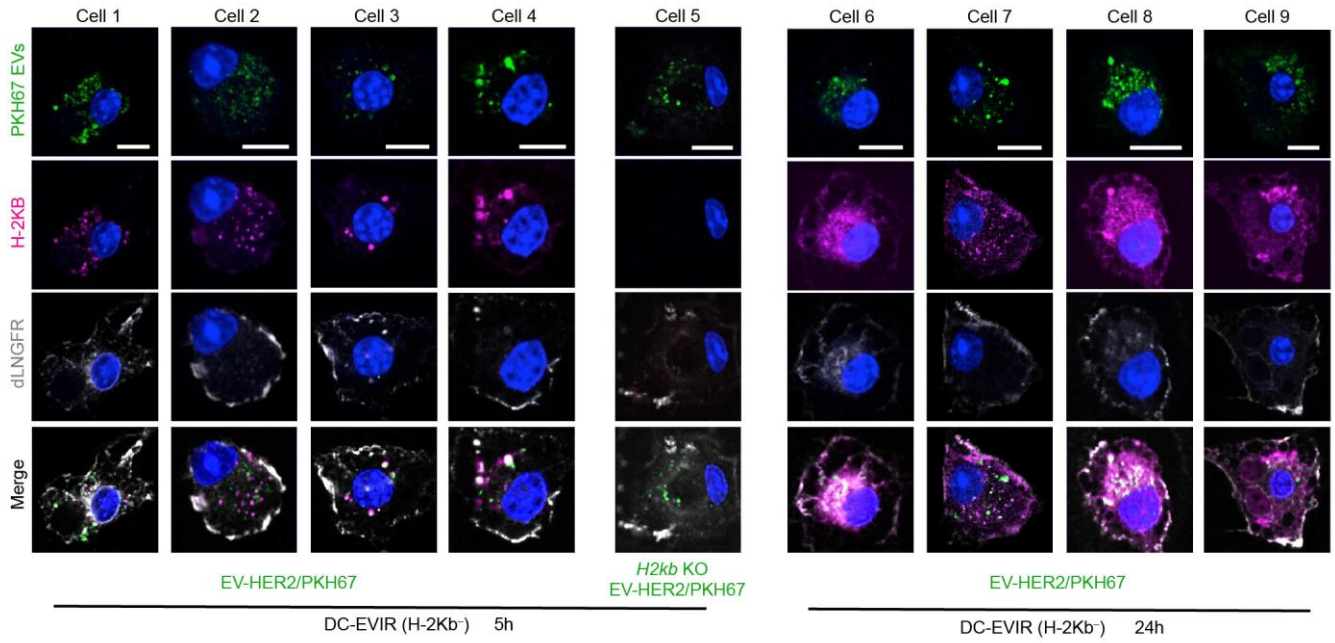

Supplementary Figure 11

An anti-HER2 EVIR promotes MHCI recycling in DCs

Representative confocal images of H-2Kb-negative DC-EVIR incubated with PKH67-labeled EV-HER2 (green), which were isolated from either *H2kb*-proficient (cells 1-4 and 6-9) or KO (cell 5) MC38 cells. Additional examples (including *H2kb* KO EVs assayed at 24 h) are shown in Figure 2c. The cells were analyzed 5 h (left panels) or 24 h (right panels) after exposure to the EVs. The cells were immunostained with antibodies against H-2Kb (magenta) and dLNGFR (white); nuclei are stained with DAPI (blue). Scale bar, 10 μm. Images are representative of 10 randomly selected cells *per* condition. Results are representative of 2 independent experiments.

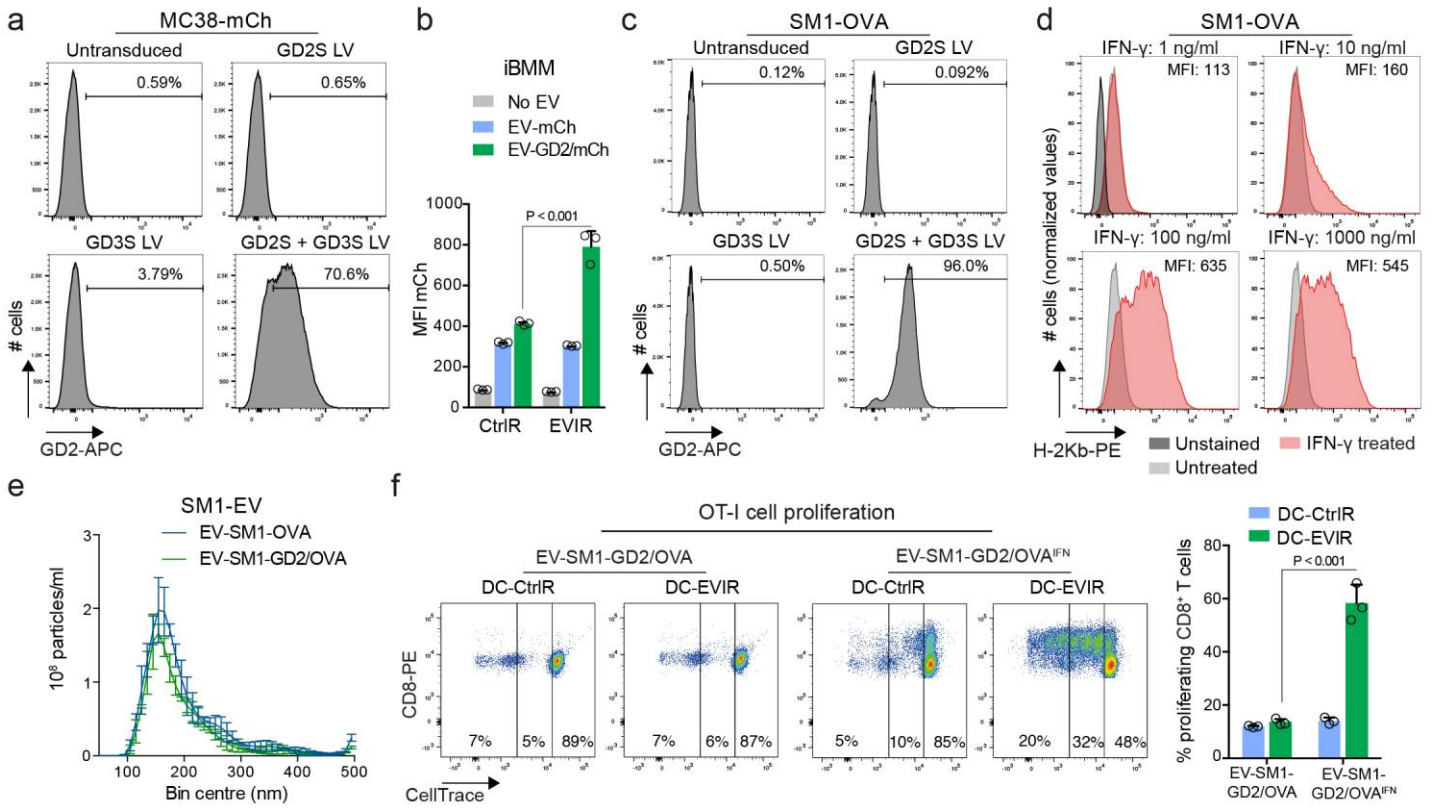

Supplementary Figure 12

An anti-GD2 EVIR enhances EV uptake by DCs and presentation of a surrogate tumor antigen to T cells

(**a**) Flow cytometry analysis of GD2 expression in MC38-mCh cells that had been transduced with the indicated GD2 synthase. The cells were analyzed once and employed in subsequent experiments.

(**b**) Flow cytometry analysis of mCh MFI in DC-CtrlR or anti-DG2 DC-EVIR untreated or treated with EV-mCh or EVs that had been isolated from GD2$^+$ MC38-mCh cells (EV-GD2/mCh). Data show mean MFI values ± SEM (n=3 independent cell cultures *per* condition); statistical analysis by two-way ANOVA with Sidak's multiple comparison test.

(**c**) Flow cytometry analysis of GD2 expression in SM1-OVA cells that had been transduced with the indicated GD2 synthase. The cells were analyzed once and employed in subsequent experiments.

(**d**) Flow cytometry analysis of H-2Kb expression in SM1-GD2/OVA cells, untreated or treated with recombinant IFNγ as indicated. The experiment was performed once.

(**e**) Size distribution of EV-SM1-OVA, either with or without GD2, as determined by NTA. Data show mean values ± SEM (n=3 technical measurements of one EV preparation *per* type). Data are representative of 2 independent EV preparations.

(**f**) Flow cytometry analysis of CD8$^+$ OT-I cell proliferation assessed by CellTrace dilution after co-culture with the indicated DCs and EVs. The left panels show representative flow cytometry dot plots (one cell culture of 3 performed *per* condition). The right panel shows the percentage of CD8$^+$ OT-I cells that completed at least 1 cell cycle. Data show mean percentages ± SEM (n=3 independent cell cultures *per* condition); statistical analysis by two-way ANOVA with Sidak's multiple comparison test.

Numerical values for the experiments with quantitative data are presented in **Supplementary Table 2**.

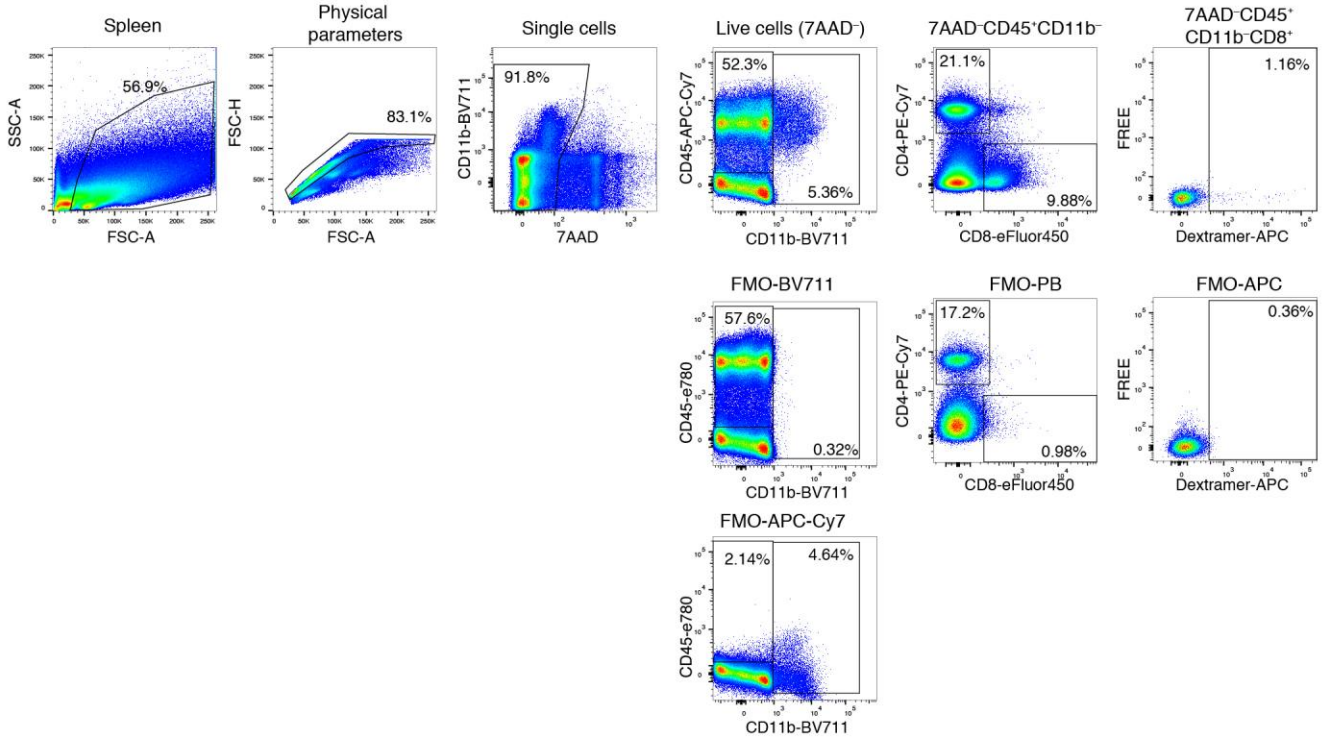

Supplementary Figure 13

Analysis of splenic T cells in tumor-bearing mice

Representative flow cytometry dot plots showing the gating strategy employed to identify dextramer^{+} CD8^{+} T cells in the spleens of MC38-bearing mice (see Figure 2e).